Development of new precursors for asymmetric preparation of α-[11C]methyl amino acids for PET

Popkov, Alexander

Chapter 4.1

Improved synthesis of the Ni(II) complex of the Schiff base of (*S*)-2-[*N*-(*N'*-benzylprolyl)amino]benzophenone and glycine

Milan Nádvorník[1] and Alexander Popkov[2]

[1]Department of General and Inorganic Chemistry, University of Pardubice, Czech Republic,
[2]University of South Bohemia, Nové Hrady, Czech Republic

Green Chem. **2002**, *4*, 71

Summary
The environmental impact of a known synthesis of the Ni complex of the Schiff base of (*S*)-2-[*N*-(*N'*-benzylprolyl)amino]benzophenone and glycine was decreased by optimisation of the ratio the starting materials; a new starting material - $Ni(NO_3)_2 \cdot 6NH_3$ was evaluated as a nickel source.

Introduction
For the preparation of non-coded and/or selectively labelled α-amino acids, several chiral glycine and alanine synthons are manufactured and marketed in bulk quantities. The most important are Seebach's[1] and Oppolzer's[2] derivatives and O'Donnell's achiral synthon,[3] for stereospecific alkylation of which an efficient chiral catalyst has been recently developed.[4] Ni(II) complexes of Schiff bases of (*S*)-2-[*N*-(*N'*-benzylprolyl)amino]benzophenone (**BPB**) and α-amino acids achieve high asymmetric induction for the synthesis of α-amino acids[5] at ambient temperature. The chiral auxilliary BPB is regenerated but excess nickel in the waste water is a potential environmental problem (Scheme 4.1.1).

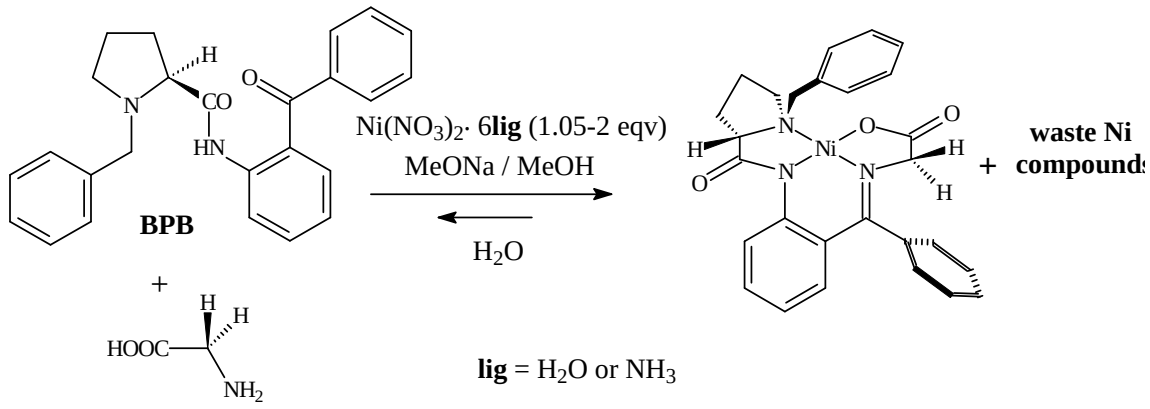

Scheme 4.1.1 Preparation of the Ni(II) complex of Schiff base of **BPB** and glycine

The complexes were developed as artificial analogues of pyridoxal 5'-phosphate (PLP)-dependent enzymes.[6] The central sodium atom of a PLP-dependent enzyme was replaced by nickel in order to form a more stable compound. In spite of the inexpensive and reliable application of these complexes, the fate of the nickel used in their preparation should be carefully controlled. Energy-consuming procedures used for removal of nickel from waste water might significantly increase cost of α-amino acids production. Nickel from the complexes is easily regenerated when a mixture of an amino acid and nickel chloride (after acidic hydrolysis) is separated on a cation-exchanger. A large amount of metal remains in the methanolic waste solution after preparation of the complexes, due to a two-fold excess of $Ni(NO_3)_2 \cdot 6H_2O$ used in a standard protocol.[7-9] This excess is necessary in order to shift the equilibrium towards complex formation.
Previous attempts to substitute nickel nitrate with nickel acetate, which bears four molecules of water in the internal coordination sphere instead of six in the nitrate, did not shift the equilibrium towards complex formation.[10]

In this work the successful synthetic application of near stochiometric amounts of $Ni(NO_3)•6H_2O$ or anhydrous $Ni(NO_3)•6NH_3$[†], minimising amount of Ni^{2+} need to be recovered from waste water, is described.

Results and discussion

In this work a two-fold excess of glycine instead of five-fold[7-9] was used in order to reduce the amount of nickel chelating amino acid in the waste water.

Experiments did not support the initial hypothesis that anhydrous $Ni(NO_3)•6NH_3$ would shift the equilibrium towards complex formation. Observed yields of complex formation starting from $Ni(NO_3)•6H_2O$ were 5-13% higher than the corresponding yields starting from $Ni(NO_3)•6NH_3$ (Table 4.1.1).

Excess of the nickel salt	**2**	**1.2**	**1.05**
Yield of the complex starting from $Ni(NO_3)_2•6NH_3$, %	64	78	67
Yield of the complex starting from $Ni(NO_3)_2•6H_2O$, %	77	88	71

Table 4.1.1 Yields of the Ni(II) complex of Schiff base of BPB and glycine depending on excess of nickel salts

When a two-fold excess of any nickel salt was used solid precipitate appeared in the reaction mixture after 90 min. With lower excesses of nickel salts no precipitates were observed. Formation of the precipitate is probably responsible for lower yields of the complexes when using a two-fold excess of a nickel salt compared with 1.2-fold. This may be due to absorption of BPB by precipitated nickel oxide/hydroxide. Work-up of the homogeneous reaction mixtures obtained with lower excesses of nickel salts is better suited to scale-up as no separation and processing of solid nickel-containing waste is necessary.

Application of the Ni(II) complex of the Schiff base of BPB and glycine for asymmetric synthesis of α-amino acids often does not require separation of the complex from unreacted BPB (for example, ref.[9]). In such cases, in spite of lower yields of the complexes, a 1.05-fold excess of nickel salt might be the best ratio. This will decrease the amount of nickel circulating in the process.

Synthesis of more sterically hindered complexes derived from α-monosubstituted glycines (*e. g.* proteinogenic α-amino acids) is in progress in order to test the new ratio of the starting compounds under more challenging conditions.

Experimental

General procedure for the synthesis of the glycine complex

2.5M MeONa/MeOH (8 ml, 20 mmol) was added to a stirred suspension of BPB (500 mg, 1.3 mmol), glycine (195 mg, 2.6 mmol) and the corresponding amount of a nickel salt (Table 4.1.1) in dry MeOH (4 ml) under argon at 55 °C. The volume of the reaction mixture was then adjusted to 15 ml with dry MeOH. After stirring at 55 °C for 90 min, the mixture was poured into 10% aqueous citric acid (100 ml), stirred and the resulting precipitate was filtered off and dried on air. The dry precipitate was purified by column chromatography using silica gel (Merck 40/63) eluted with chloroform.[‡] Yields of complex formation are given in the Table 4.1.1. ^{1}H and ^{13}C-NMR data have been reported previously[11].

Acknowledgement
The authors are grateful to Dr Nicholas Gillings for linguistic corrections.

Notes and references
† $Ni(NO_3)•6NH_3$ for this work was prepared by bubbling NH_3 gas through a cold methanolic solution of $Ni(NO_3)•6H_2O$ and filtering off the resulting precipitate. Aqueous ammonia may be also used instead of NH_3 gas, in this case content of water in the internal coordinational sphere of $Ni(NO_3)•6NH_3$ will be higher.

‡ As chloroform is known to be a human carcinogen, for preparative applications a gradient elution using $CH_2Cl_2 \rightarrow CH_2Cl_2 : Me_2CO$=7:1 or toluene → toluene : Me_2CO=2:1 is strongly recommended.

1 D. Seebach, A. R. Sting and M. Hoffmann, *Angew. Chem., Int. Ed.*, 1996, **35**, 2708
2 W. Oppolzer, R. Moretti and C. Zhou, *Helv. Chim. Acta*, 1994, **77**, 2363
3 M. J. O'Donnell, *Aldrichimica Acta*, 2001, **34**, 3
4 T. Ooi, M. Takeuchi, M. Kameda and K. Maruoka, *J. Am. Chem. Soc*., 2000, **122**, 5228
5 Y. N. Belokon, *Pure Appl. Chem.*, 1992, **64**, 1917
6 H. C. Dunathan, *Adv. Enyzmol. Relat. Areas Mol. Biol.*, 1971, 79
7 Y. N. Belokon, V. I. Tararov, V. I. Maleev, T. F. Saveleva and M. G. Ryzhov, *Tetrahedron: Asymmetry*, 1998, **9**, 4249
8 Y. N. Belokon, V. I. Bakhmutov, N. I. Chernoglazova, K. A. Kochetkov, S. V. Vitt, N. S. Garbalinskaya and V. M. Belikov *J. Chem. Soc., Perkin Trans. 1*, 1988, 305
9 V. A. Soloshonok, D. V. Avilov, V. P. Kukhar, V. I. Tararov, T. F. Saveleva, T. D. Churkina, N. S. Ikonnikov, K. A. Kochetkov, S. A. Orlova, A. P. Pysarevsky, Y. T. Struchkov, N. I. Raevsky and Y. N. Belokon, *Tetrahedron: Asymmetry*, 1995, **6**, 1741
10 J. Jirman and A. Popkov, *Collect. Czech. Chem. Commun*., 1994, **59**, 2103.
11 A. Popkov, J. Jirman, M. Nádvorník and P. A. Manorik, *Collect. Czech. Chem. Commun*., 1998, **63**, 990

Chapter 4.2

Syntheses, X-ray, MS^n, NMR structure determination of nickel(II) complexes of Schiff bases of (*S*)-*N*-(2-benzoylphenyl)-1-benzyl-pyrrolidine-2-carboxamide and aromatic α-amino acids

Milan Nádvorník[1], Vratislav Langer[2], Robert Jirásko[3], Michal Holčapek[3], Tomáš Weidlich[4] , Antonín Lyčka[5] and Alexander Popkov[6]

[1]Department of General and Inorganic Chemistry, University of Pardubice, Czech Republic, [2]Chalmers University of Technology, Göteborg, Sweden, [3]Department of Analytical Chemistry, Pardubice University, Czech Republic, [4]Institute of Environment Protection, University of Pardubice, Czech Republic, [5]Research Institute for Organic Syntheses, Rybitví, Czech Republic, [6]Department of Nuclear Medicine and Molecular Imaging, University Medical Center Groningen, University of Groningen, The Netherlands

Submitted for publication

Summary
A preparative procedure for the synthesis of an important chiral synthon of side-chain protected tyrosine was developed and optimised for the minimisation of nickel salts waste. While preparing a similar side-chain protected tryptophan synthon, an unexpected low stability was found of the Boc-protective group of the tryptophan aromatic nitrogen during purification on silica gel. X-Ray crystal structure determination, tandem mass spectrometry (MS/MS) and NMR were applied for the elucidation of structures of prepared complexes and by-products. Stereochemistry of products of α-methylation of the complexes was accessed using a model tyrosine-derived compound.

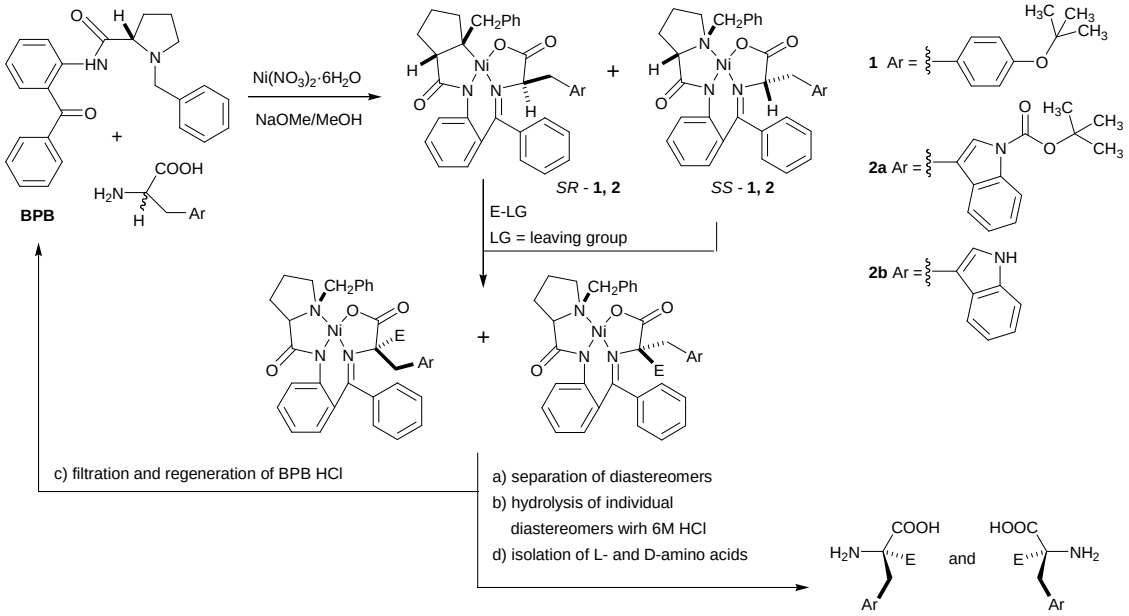

Scheme 4.2.1 Preparation and application of aromatic amino acids synthons

Introduction
Ni(II) complexes of Schiff bases of (*S*)-*N*-(2-benzoylphenyl)-1-benzylpyrrolidine-2-carboxamide (BPB) and α-amino acids were developed as artificial analogues of pyridoxal 5'-phosphate (PLP)-dependent enzymes.[1] Their preparative applications for stoichiometric, asymmetric synthesis of α-amino acids are being perfected by a number of groups worldwide.[2] Significant steps have been made in reducing the environmental impact of the complexes' high-scale application. The most important feature is that BPB itself was initially designed as a re-usable enzyme-like auxilliary.[3] In the synthesis of BPB no chromatographic steps are used.[4] Recently, an improved synthesis of BPB was published in which work with the lacrymatory alkylating agent benzylchloride was avoided. In a catalytic process, less toxic benzaldehyde was used without any reduction of isolated product.[5] Preparation of the complexes from BPB, nickel nitrate, sodium methoxide and various α-amino acids results in the release of nickel to waste water. For the most frequently used complex derived from the simplest α-amino acid glycine, a modified procedure was developed.[6] It allowed for a significant decrease in the amount of nickel in waste water. The question arises as to whether it is possible to reduce the amount of nickel in waste water in the preparation of complexes derived from other proteinogenic α-amino acids. Such complexes are being prepared in lower

amounts than the complex derived from glycine, but their consumption is increasing, *e. g.* for preparation of α-methyl amino acids for positron emission tomography[7] or other quaternary α-amino acids.[8] In this work we investigated the dependence of the yields of the complexes derived from side-chain protected tyrosine or tryptophan on the amount of nickel nitrate and amino acid employed. Both amino acids' side chains were protected by *tert*-Bu- and Boc-protective groups, respectively (Scheme 4.2.1). Compatibility of these standard side chain protective groups for Fmoc-strategy of peptide synthesis was assessed in relation to the reaction conditions used for preparation of the complexes. Stereochemistry of products of α-methylation of the complexes was accessed using a model complex derived from tyrosine protected by a methyl group in the side chain.

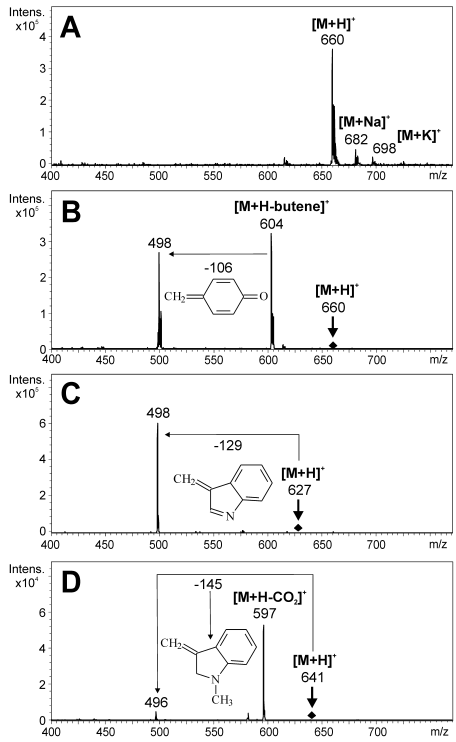

Figure 4.2.1 Positive-ion electrospray ionization mass spectra:
A/ First-order spectrum of 1,
B/ MS/MS spectrum of ion m/z 660 $[M+H]^+$ for 1,
C/ MS/MS spectrum of ion m/z 627 $[M+H]^+$ for 2b,
D/ MS/MS spectrum of ion m/z 641 $[M+H]^+$ for 3.

Results and discussion

Ratios of starting compounds for the preparation of complexes were chosen from a previous optimisation protocol of the ratio of starting compounds for preparation of the glycine-derived complex.[6] Twenty percent excess of nickel nitrate to BPB was predicted to be optimal for both maximisation of the yield of complexes and minimisation of the amount of nickel in waste water. Five and fifty percent excess were also tested (Table 4.2.1). Unlike glycine used in previous work, both side-chain protected amino acids are relatively expensive. Thus, the

previously applied two-fold excess of amino acid was considered to be uneconomical. Ten, twenty and forty percent excess of amino acid to BPB were tested (Table 4.2.1). Experiments demonstrated that in this particular case the Boc-protective group of the indole residue nitrogen is unstable during chromatographic purification on silica gel. A significant amount of the complex derived from protected tryptophan lost the protective group during quick preparative TLC purification of an analytical sample. Clean deprotection was observed in all four preparative syntheses followed by time-consuming purification of the product by column chromatography on silica gel. No observations of low stability of indole nitrogen Boc-protected derivatives of tryptophan[9] were found in the literature. Deprotection was confirmed by NMR, MS/MS and X-ray data. In order to demonstrate the necessity of including the protective group for the preparation of quaternary α-amino acids via *C*-methylation of carbanion generated from tertiary precursor,[7] a sample of deprotected complex was methylated with an excess of CH_3I/KOH in 1,3-dimethylimidazolidin-2-one. This resulted in pure *N*-methylated product without any traces of the *C*-methylated product as confirmed by both MS^n and X-ray data (Scheme 4.2.2, Figures 4.2.1C, 4.2.1D, 4.2.2 and 4.2.3).

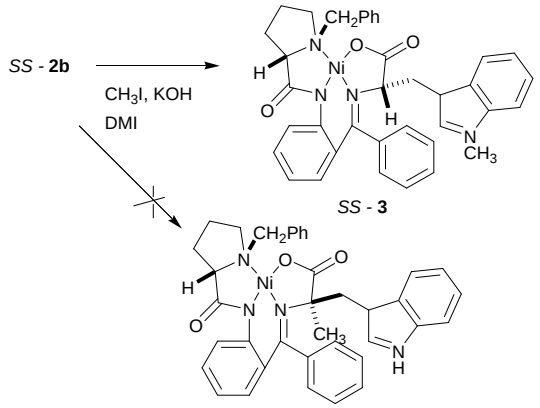

Scheme 4.2.2 *C*- versus *N*-methylation of the tryptophan synthon

Development of an alternative purification method is underway. *tert*-Butyl protection of the phenolic group of tyrosine is perfectly compatible with the reaction conditions used and with column chromatography on silica gel (Fig. 4.2.1B).

Typical ions in first-order positive-ion ESI mass spectra are protonated molecules and adducts with alkali metal ions, such as $[M+Na]^+$ and $[M+K]^+$ (Fig. 4.2.1A). The presence of these ions was used for the determination of molecular weights of all analysed compounds (see Experimental part for more details). Based on the determination of molecular weights, the presence or absence of a protective group or another substituent on the aromatic nitrogen (for tryptophan) or oxygen atom (for tyrosine side-chains) can be recognised. Furthermore, the presence of a protective group can be confirmed by typical neutral losses associated with a particular group. In the case of complex 1, the typical neutral losses are Δm/z 56 (butene) and 106 (see Fig. 4.2.1B). For deprotected complex 2b, the characteristic neutral loss is Δm/z 129 (see Fig. 4.2.1C). However for *N*-methylated complex 3, the neutral loss is Δm/z 145 (see Fig. 4.2.1D).

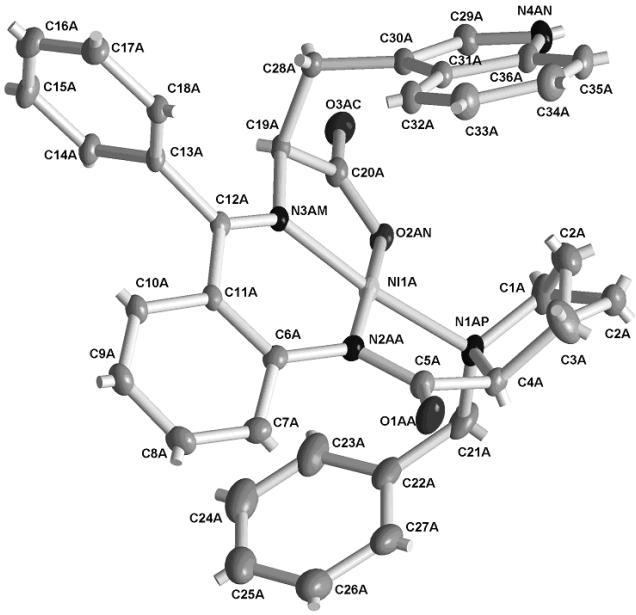

Figure 4.2.2 Full-color in appendix. The numbering scheme for *SS* – **2b**, the first complex, with atomic displacement ellipsoids at 30% probability level. Note disorder of C2A. Hydrogens are omitted for clarity.

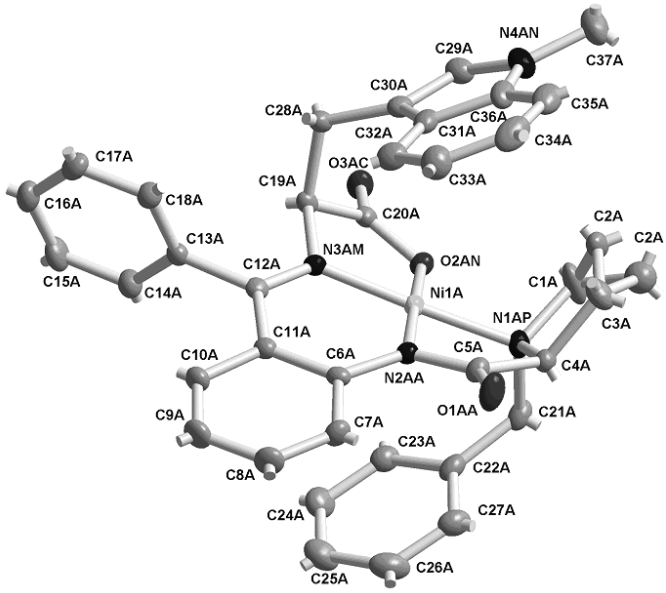

Figure 4.2.3 Full-color in appendix. The numbering scheme for *SS* – **3**, the first complex, with atomic displacement ellipsoids at 30% probability level. Note disorder of C2A. Hydrogens are omitted for clarity.

Both complexes *SS* – **2b** and *SS* - **3** crystallize with solvent molecules in the crystalline lattice. The crystals loose some solvent molecules during drying in air at ambient temperature. For such crystallosolvates, X-ray crystallography of shock-frozen single crystals is an informative method of structure characterisation.

***SS* – 2b**

There are 2 crystallographically different complexes co-crystallized with 3 benzene molecules in the asymmetric unit. Both complexes suffer from disorder at C2 atoms and one of them even has disorder of the phenyl group, see Fig. 4.2.2 and Fig 4.2.4 (in Supplementary Information). There are hydrogen bonds in the structure producing an helical arrangement of the complexes, see Figures 4.2.5 and 4.2.6 (in Supplementary Information). Packing in the unit cell along the monoclinic b-axis is in Fig. 4.2.7 (in Supplementary Information).

***SS* - 3**

There are 2 crystallographically different complexes co-crystallized with 2 benzene and 2 water molecules in the asymmetric unit. Again, both complexes suffer from disorder at C2 atoms (see Fig. 4.2.3 and Fig. 4.2.8) (in Supplementary Information). There are hydrogen bonds in the structure producing an helical arrangement of the complexes, see Fig. 4.2.9 and 10. Packing in the unit cell along the orthorhombic b-axis is shown in Fig. 4.2.11.

For both structures, the absolute structures were unambiguously determined. All nickel complexes show square-planar co-ordination geometry with small pyramidal distortions.

$Ni(NO_3)_2 \cdot 6H_2O$ excess	Amino acid excess	BPB	Yield of complex 1 (sum of diastereomers)	Yield of complex 2b (sum of diastereomers)
1.05	1.1	1	57	55
1.2	1.2	1	79	61
1.2	1.4	1	83	86
1.5	1.4	1	87	79

Table 4.2.1 Yields of complexes (both *SS* and *SR* diastereomers) depending on ratios of the starting compounds used

Five and ten percent excess of nickel nitrate and amino acid, respectively, led to poor yields of both complexes (Table 4.2.1). This result corresponds with the low yield of glycine-derived complex obtained with five percent excess of nickel nitrate.[6] As expected, twenty percent excess of nickel nitrate led to high yield of both complexes. With such an excess of nickel salt, a higher excess of amino acid gave a slightly higher excess of complex **1** derived from tyrosine, and led to significantly higher yield of the complex derived from tryptophan (**2a→2b**) (Table 4.2.1). Lower yield of this complex in the case when fifty percent excess of nickel nitrate was used, is consistent with previously observed relationship between an excess of nickel nitrate used and yields of the complexes derived from glycine. Diastereomeric excess of (*SS*)-diastereomers in all cases was >95%. Minor (*SR*)-diastereomers were collected and partially characterised. Due to epimerisation of the amino acid stereogenic centre in basic conditions, in further alkylation reaction mixtures of both diastereomers could be used without separation.[8]

Due to poor preparative TLC separation of diastereomeric products of α-methylation of complex *SS* – **3,** its analogue complex *SS* - **4** (carrying methyl protective group of the side chain instead of *tert*-Bu) was used to access stereochemistry of products of α-methylation of such complexes. These diastereomeric products of methylation *SS* – **5** and *SR* – **5** are separable by preparative TLC on silicagel while for separation of many other similar diastereomers expensive preparative HPLC is necessary. Stereochemistry of the diastereomers of **5** was assesed by circular dichroism (CD) and ^{13}C NMR spectroscopy:

- Two intensive peaks were observed in the ^{13}C NMR spectrum of the reaction mixture after alkylation of *SS* - **4** with $^{13}CH_3I$/KOH in DMI (Scheme 4.2.3): minor at 29.3 ppm and major at 28.5 ppm. According to integral intensities of peaks in ^{13}C NMR spectra, the diastereomeric excess of methylation was 6.9 %;
- Two fractions were obtained after preparative TLC separation of the reaction. The first fraction giving a main ^{13}C NMR peak at 29.3 ppm was associated with the minor diastereomer. The second fraction where the main peak was at 28.5 ppm, was associated with the major diastereomer;
- CD spectra of starting *SS* - **4** and both diatereomers of **5** were recorded. Cotton effects in the spectra of both *SS* - **4** and the first TLC fraction (minor diastereomer) of **5** were similar in two areas (650-480 nm and 480-360 nm). Cotton effect in the spectrum of the second TLC fraction (major diastereomer) of **5** in the range 480-360 nm had an opposite sign. Based on these CD data, the *SS* configuration was assigned to the first fraction (minor diastereomer) and the *SR* configuration was assigned to the second fraction (major diastereomer). This assignment is consistent with proposed predominance of *Si*-alkylation leading to major formation of *SR* – **5** (Scheme 4.2.3).

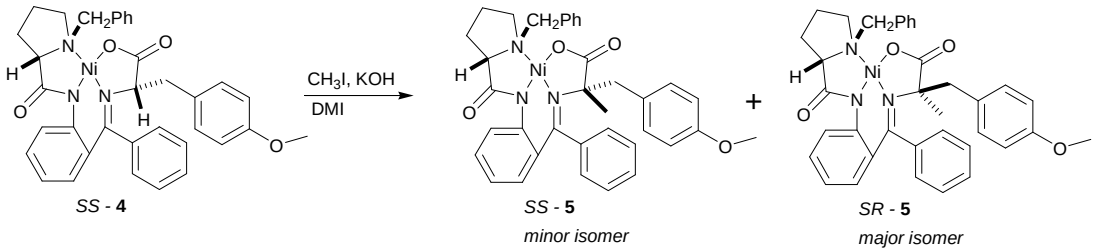

Scheme 4.2.3 *C*- versus *N*-methylation of the tryptophan synthon

Experimental

The ^1H and ^{13}C NMR spectra were obtained in $CDCl_3$ solutions using a Bruker AMX-360 spectrometer equipped with a multinuclear 5 mm tunable probe with ^1H at 360.13 MHz and ^{13}C at 90.56 MHz, respectively. ^1H NMR chemical shifts are expressed in parts per million (ppm) downfield from tetramethylsilane as an internal standard. Coupling constants *J* are given in Hz. ^{13}C NMR chemical shifts are given with respect to the solvent signal (δ = 77 ppm). Data are given in the following order: δ value (multiplicity (s, singlet; d, dublet; dd dublet of dublet; m, multiplet; t, triplet; bs, broad singlet), number of protons).

Positive-ion electrospray ionization (ESI) mass spectra were measured on an Esquire 3000 ion trap analyzer (Bruker Daltonics, Bremen, Germany) in the range m/z 50 - 1000. The samples were dissolved in 100% acetonitrile and analyzed by direct infusion at the flow rate 5 μl/min.

The selected precursor ions were further analyzed by MS/MS analyses under the following conditions: the isolation width m/z = 8, the collision amplitude (in the range 0.8 - 1.0 V depending on the precursor ion stability), the ion source temperature (300°C), the tuning parameter compound stability (100%), the flow rate and the pressure of nitrogen (4 l/min and 10 psi), respectively. The elemental composition of the complexes *SS* – **1** and *SS* – **2b** was confirmed on an orthogonal hybrid quadrupole time-of-flight (QTOF) mass spectrometer fitted with electrospray ionization source (Bruker Daltonics). The instrument was externaly calibrated using ESI tunning mix before the measurement. The samples were dissolved in acetonitrile and analyzed by direct infusion at the flow rate of 3 µl/min. Interface parameters were set as follows: capillary voltage -4.5 kV, drying temperature 200 °C, the flow rate and pressure of nitrogen were 4 l/min and 0.4 bar, respectively. For the recording of exact masses, QTOF data were acquired by summation of 50000 scans with 10 rolling averages. The typical ions observed in the first-order positive-ion mass spectra were $[M+H]^+$, $[M+Na]^+$ and $[M+K]^+$ and the elemental composition was confirmed by comparison of experimental and theoretical values for all studied compounds. Table 2 shows mass accuracies for monoisotopic masses, mean mass accuracies correspond to the mean value for all isotopic peaks and the sigma is a combined value for the standard deviation of masses and intensities for all peaks.

Table 4.2.2 Mass accuracies and sigma values used

		$[M+H]^+$	$[M+Na]^+$	$[M+K]^+$
Complex *SS* – **1** $C_{38}H_{39}N_3O_4Ni$	Mass accuracy [ppm]	1.0	0.3	0.7
	Mean mass accuracy [ppm]	-1.4	-0.3	0.6
	Sigma	0.015	0.005	0.025
Complex *SS* – **2b** $C_{36}H_{32}N_4O_3Ni$	Mass accuracy [ppm]	1.5	0.6	0.0
	Mean mass accuracy [ppm]	-0.7	0.548	0.0
	Sigma	0.025	0.013	0.024

The elemental composition of the complexes *SS* – **5** and *SR* – **5** was confirmed on a sector mass spectrometer fitted with electron-impact ionization source (VG Analytical) by a commercial analytical laboratory.

Diffraction data were collected using a Siemens SMART CCD diffractometer with Mo-Ka radiation (λ = 0.71073 Å, graphite monochromator). The crystals were cooled to 173(2) K by a flow of nitrogen gas using the LT-2A device. A full sphere of reciprocal space was scanned by 0.3 steps in ω with a crystal-to-detector distance of 3.97 cm. Preliminary orientation matrices were obtained from the first frames using SMART. The collected frames were integrated using the preliminary orientation matrices which were updated every 100 frames. Final cell parameters were obtained by refinement of the positions of reflections with I > 10σ (I) after integration of all the frames using SAINT software.[9] The data were empirically corrected for absorption and other effects using the SADABS program.[11] The structures were solved by direct methods and refined by full-matrix least squares analysis on all |F2| data using SHELXTL software. The crystallographic and refinement data are summarized in Tables 4.2.3 and 4. The hydrogen bonding geometrical parameters are summarized in Tables 4.2.5 and 4.2.6 (in Supplementary Information). Selected bond lengths, selected bond angles and their estimated standard deviations are listed in Tables 4.2.7 and 4.2.8 (in Supplementary Information). The molecular graphics (Figures 4.2.2-4.2.11) were prepared using the program DIAMOND.[13]

Circular dichroism spectra were recorded using a Jasco J-715 spectropolarimeter.

Table 4.2.3 Crystal data and structure refinement for *SS* – **2b**

Empirical formula	$C_{43}\ H_{42}\ N_4\ Ni\ O_4$	
Formula weight	737.52	
Temperature	173(2) K	
Wavelength	0.71073 Å	
Crystal system	Orthorhombic	
Space group	$P2_12_12_1$	
Unit cell dimensions	a = 13.9338(2) Å b = 14.6081(2) Å c = 36.1605(5) Å	α= 90° β= 90° γ = 90°
Volume	7360.34(18) Å3	
Z	8	
Density (calculated)	1.331 Mg/m3	
Absorption coefficient	0.576 mm-1	
F(000)	3104	
Crystal size	0.44 x 0.26 x 0.19 mm3	
Theta range for data collection	2.10 to 25.00°	
Index ranges	-16<=h<=16 -17<=k<=17 -43<=l<=43	
Reflections collected	77400	
Independent reflections	12942 [R(int) = 0.0583]	
Completeness to theta = 30.56°	99.8 %	
Absorption correction	multi-scan	
Max. and min. transmission	0.8984 and 0.7857	
Refinement method	Full-matrix least-squares on F2	
Data / restraints / parameters	12942 / 6 / 972	
Goodness-of-fit on F2	1.026	
Final R indices [I>2sigma(I)]	R1 = 0.0518 wR2 = 0.1268	
R indices (all data)	R1 = 0.0593 wR2 = 0.1320	
Absolute structure parameter	0.025(13)	
Largest diff. peak and hole	1.141 and -0.378 e.Å-3	

General procedure for the synthesis of complexes

2.47M MeONa/MeOH (7.9 ml, 19.5 mmol) was added to a stirred suspension of BPB (500 mg, 1.3 mmol) and the corresponding amount of nickel nitrate and protected amino acid (Table 1) in dry MeOH (4 ml) under argon at 50 °C. The volume of the reaction mixture was then

adjusted to 20 ml with dry MeOH. After stirring at 55 °C for 30 min, the mixture was poured into 0.7% aqueous citric acid (300 ml), stirred and the resulting precipitate was filtered off, washed with water on a filter and dried on air. The dry precipitate was purified by column chromatography using silica gel (Merck 40/63) and eluted with chloroform.† First red fractions containing minor (*SR*)-diastereomers and second red fractions containing major (*SS*)-diastereomers were collected. Yields of complex formation are given in the Table 1. Complexes *SS* – **2b** and *SS* - **3** were purified by preparative TLC followed by crystallisation from a (wet) acetone-benzene mixure which gave a crystallosolvat. Resulting red single crystals are unstable in air at ambient temperature; they loose benzene (and water in the case of *SS* - **3**) and decompose within tens of minutes.

(*SR*)-diastereomer of complex 2b. δ_H (360.13 MHz, $CDCl_3$; Me_4Si) 1.36 (2H, m), 1.84 (1H, m), 2.21(1H, m), 2.30(1H, m), 3.07(5H, m), 3.64 (1H, m), 4.30 (1H, t), 6.76 (1H, m), 6.84 (1H, m), 7.05 (1H, m), 7.10 (3H, m), 7.15 (1H, m), 7.20 (1H, m), 7.31 (4H, m), 7.38 (2H, d), 7.49 (2H, m), 7.55(2H, m), 8.39 (1H, br s, NH), 8.52 (1H, d). δ_C (90.57 MHz, $CDCl_3$) 23.57 CH_2, 30.92 CH_2, 31.11 CH_2, 54.91 CH_2, 58.66 CH_2, 68.30 CH, 72.25 CH, 110.35 C_q, 111.17 CH, 120.11 CH, 120.44 CH, 120.67 CH, 122.50 CH, 123.76 CH, 124.81 CH, 126.08 C_q, 127.19 CH, 128.16 CH, 128.55 2xCH, 128.67 CH, 128.72 C_q, 128.81 CH, 129.27 CH, 129.69 CH, 131.76 C_q, 131.90 2xCH, 132.59 CH, 133.76 CH, 134.83 C_q, 136.57 C_q, 143.23 C_q, 170.96 C_q, 179.22 C_q, 181.88 C_q.

(*SS*)-diastereomer of complex 2b. δ_H (360.13 MHz, $CDCl_3$; Me_4Si) 1.42 (1H, m), 1.79 (2H, m), 1.89 (1H, m), 2.11 (1H, m), 2.80 (1H, m), 3.07 (1H, dd, A part of AMX system), 3.21 (1H, dd, M part of AMX system), 3.36 (1H, dd, X part of AMX system), 3.40 (1H, d, A part of AB system of CH_2Ar, $^2J_{AB}$ 12.6), 4.21 (1H, d, B part of AB system of CH_2Ar, $^2J_{AB}$ 12.6), 4.35 (1H, t), 6.74 (2H, m), 6.92 (2H, m), 7.01 (1H, t), 7.19 (3H, m), 7.36 (6H, m), 7.56 (2H, m), 8.01 (2H, d), 8.30 (1H, d), 8.93 (1H, br s, NH). δ_C (90.57 MHz, $CDCl_3$) 22.58 CH_2, 30.22 CH_2, 30.52 CH_2, 56.91 CH_2, 63.12 CH_2, 70.27 CH, 71.55 CH, 109.41 C_q, 111.25 CH, 119.50 CH, 119.78 CH, 120.48 CH, 122.10 CH, 123.35 CH, 124.42 CH, 126.12 C_q, 127.17 CH, 127.90 CH, 128.26 Cq, 128.63 2xCH, 128.65 CH, 128.70 CH, 128.95 CH, 129.58 CH, 131.42 2xCH, 132.20 CH, 133.16 C_q, 133.45 CH, 134.03 C_q, 136.50 C_q, 142.68 C_q, 170.73 C_q, 179.47 C_q, 180.08 C_q. Positive-ion mass spectra: m/z 665 $[M+K]^+$, m/z 649 $[M+Na]^+$, m/z 627 ($[M+H]^+$, 100%), m/z 498 $[M+H-129]^+$. MS/MS of m/z 627: m/z 498 $[M+H-129]^+$. For the single crystal structure, see Fig. 4.2.2.

(*SS*)-diastereomer of complex 3. Positive-ion mass spectra: m/z 679 $[M+K]^+$, m/z 663 ($[M+Na]^+$, 100%), m/z 641 $[M+H]^+$. MS/MS of m/z 641: m/z 597 $[M+H-CO2]^+$, m/z 496 $[M+H-145]^+$. For the single crystal structure, see Fig. 4.2.3.

(*SR*)-diastereomer of complex 1. δ_H (360.13 MHz, $CDCl_3$; Me_4Si) 1.34 (9H, s), 1.80 (1H, m), 1.99 (1H, m), 2.38 (1H, m), 2.49 (1H, m), 2.60 (1H, m), 2.89 (1H, dd, A part of AMX system), 3.13 (2H, m, M part of AMX system and one of proline protons), 3.32 (1H, dd, X part of AMX system), 3.45 (1H, d, A part of AB system of CH_2Ar, $^2J_{AB}$ 12.7), 4.22 (1H, t), 4.28 (1H, d, B part of AB system of CH_2Ar, d, 1H, $^2J_{AB}$ 12.7), 6.65 (2H, m), 6.70 (1H, m), 6.97 (2H, m), 7.03 (2H, m), 7.16 (2H, m), 7.26 (1H, m), 7.31 (2H, t), 7.38 (1H, m), 7.51 (2H, m), 8.03 (2H, d), 8.23 (1H, d). δ_D (90.57 MHz, $CDCl_3$) 23.23 CH_2, 28.84 3xCH_3, 30.80 CH_2, 39.54 CH_2, 57.32 CH_2, 63.22 CH_2, 70.39 CH, 71.66 CH, 78.28 C_q, 120.55 CH, 123.34 CH, 123.93 2xCH, 126.12 C_q, 127.16 CH, 127.84 CH, 128.74 2xCH, 128.76 CH, 128.80 CH, 128.95 CH, 129.64 CH, 130.10 C_q, 130.95 2xCH, 131.49 2xCH, 132.28 CH, 133.25 C_q, 133.49 CH, 134.09 C_q, 142.77 C_q, 155.21 C_q, 171.00 C_q, 178.62 C_q, 180.44 C_q.

(*SS*)-diastereomer of complex 1. δ_H (360.13 MHz, $CDCl_3$; Me_4Si) 1.28 (1H, m), 1.33 (9H, s), 1.53 (1H, m), 1.94 (1H, m), 2.14 (1H, m), 2.68 (1H, m), 2.85 (1H, dd, A part of AMX system), 2.98 (1H, dd, M part of AMX system), 3.48 (1H, d, A part of AB system of CH_2Ar $^2J_{AB}$ 13.8), 3.54 (1H, dd, X part of AMX system), 3.74 (1H, d, B part of AB system of CH_2Ar $^2J_{AB}$ 13.8Hz), 4.05 (1H, m), 4.20 (1H, t), 6.77 (2H, m), 6.96 (1H, d), 7.07 (2H, m), 7.17 (2H, m), 7.30 (1H, m), 7.38 (3H, m), 7.51 (6H, m), 8.43 (1H, d). δ_C (90.57 MHz, $CDCl_3$) 23.60 CH_2, 28.81 3xCH_3, 31.19 CH_2, 39.41 CH_2, 56.50 CH_2, 60.59 CH_2, 69.14 CH, 71.72 CH, 78.44 C_q, 120.81 CH, 123.80 CH, 124.12 2xCH, 126.36 C_q, 127.19 CH, 127.89 CH, 128.68 2xCH, 128.78 CH, 128.81 CH, 129.23 CH, 129.79 CH, 130.39 C_q, 131.54 2xCH, 132.08 2xCH, 132.51 C_q, 132.58 CH, 133.73 CH, 134.16 C_q, 143.08 C_q, 155.29 C_q, 171.01 C_q, 178.42 C_q, 181.74 C_q. Positive-ion mass spectra: m/z 698 $[M+K]^+$, m/z 682 $[M+Na]^+$, m/z 660 ($[M+H]^+$, 100%). MS/MS of m/z 660: m/z 604 $[M+H\text{-butene}]^+$, m/z 498 $[M+H\text{-butene-106}]^+$.

(*SS*)-diastereomer of complex 4 was prepared according to the published procedure.[14]

α-(^{13}C)Methylation of (*SS*)-4

Under an atmosphere of Ar at 20°C to a solution of TyrK (62 mg, 0.1 mmol) in DMI (3 ml), excess of KOH and $^{13}CH_3I$ (63 μl, 1 mmol) were added and the reaction mixture was stirred for 30 min. The reaction mixture was poured into 10% aqueous citric acid (50 ml), stirred and the resulting red oil was filtered off. The filter was dried and extracted with chloroform. The extract was evaporated in vacuo. The diastereomeric excess was calculated based on the ratio of the integral intensities of the $^{13}CH_3$- signals in the ^{13}C NMR spectra of the mixtures of the diastereomers. *SS*-5 and *SR*-5 were separated by preparative TLC using silica gel (Merck 60H) eluted with CH_2Cl_2. Yield of *SS*-5 and *SR*-5 waries (40-70%) depends on dryness of KOH used for the synthesis.

(*SR*)-diastereomer of complex 5. The first fraction, red solidified oil, (*SS*)-5. The obtained complex was then purified by chromatography on Sephadex LH-20 with toluene: MeOH = 2:1. ^{1}H NMR (500.13 MHz, $CDCl_3$): 8.10 (d, 1H), 7.99 (m, 2H), 7.47 (m, 1H), 7.37 (m, 1H), 7.30 (m, 5H) 7.25 (s, 1H), 7.20 (m, 1H), 7.10 (m, 2H), 6.98 (m, 3H), 6.59 (s, 2H), 4.29 (d, 1H) and 3.54 (d, 1H) (AB system of -CH_2Ar, ^{2}J(H, H) = 12.6 Hz), 3.81 (s, 3H, OCH_3), 3.27 (m, 1H), 3.10 (m, 2H), 2.34 (m, 1H), 2.24 (m, 2H), 2.10 (m, 1H), 1.91 (m, 1H), 1.70 (m, 1H), 1.13 (d, ^{1}J(H, C) = 130 Hz, 3H, CH_3). ^{13}C NMR (125.77 MHz, $CDCl_3$): 29.32. Calculated mass for $C_{35}{}^{13}CH_{35}N_3O_4Ni$ $[M]^+$ = 632.2015. High resolution EI-MS found $[M]^+$ = 632.2015.

(*SR*)-diastereomer of complex 5. The second fraction, red crystals, (*SR*)-5. The obtained complex was then purified by chromatography on Sephadex LH-20 with toluene: MeOH = 2:1. M. p. 274-276 °C (from acetone). ^{1}H NMR (500.13 MHz, $CDCl_3$): 7.86 (d, 1H), 7.75 (m, 2H), 7.51 (m, 1H), 7.41 (m, 2H), 7.33 (m, 2H), 7.25-7.01 (m, 6H), 6.94 (m, 2H), 6.70 (m, 1H), 6.62 (t, 1H), 4.13 (d, 1H) and 3.39 (d, 1H) (AB system of -CH_2Ph, ^{2}J(H, H) = 14.3 Hz), 3.72 (s, 3H, OCH_3), 3.32 (m, 1H), 3.06 (m, 1H), 2.99 (d, 1H) and 2.86 (d, 1H) (AB system of -CH_2Ar, ^{2}J(H, H) = 14.7 Hz), 2.32 (m, 1H), 2.13 (m, 2H), 1.91 (m, 1H), 1.42 (d, ^{1}J(H, C) = 130 Hz, 3H, CH_3). ^{13}C NMR (125.77 MHz, $CDCl_3$): 28.58. Calculated mass for $C_{35}{}^{13}CH_{35}N_3O_4Ni$ $[M]^+$ = 632.2015. High resolution EI-MS found $[M]^+$ = 632.2018.

NMR data are consistent with published data for similar complexes derived from α-methylphenylalanine or α-methyltyrosine-(OBn).[8] Half-minute intervals between pulses were applied for recording of integral intensities of signals in ^{13}C NMR spectra.

Conclusions

A preparative procedure for the synthesis of a practically important chiral synthon of side-chain protected tyrosine was developed and optimised for maximum reduction of nickel salts waste. While preparing a similar side-chain protected tryptophan synthon, unexpected low stability of Boc-protective group of tryptophan aromatic nitrogen was found during purification on silica gel. Stereochemistry of diastereomers of α-methylated complexes was disclosed using model compounds.

Acknowledgements

The authors thank Mr Joe Bird and Dr Katrin Probst for language corrections and acknowledge the support of project grants MSM0021627501 and MSM0021627502 sponsored by the Ministry of Education, Youth and Sports of the Czech Republic

Notes and references

‡ As chloroform is known to be a human carcinogen, for preparative applications a gradient elution using $CH_2Cl_2 \rightarrow CH_2Cl_2 : Me_2CO$=7:1 or toluene → toluene : Me_2CO=2:1 is strongly recommended.

1. H. C. Dunathan, *Adv. Enyzmol. Relat. Areas Mol. Biol.*, 1971, 79.
2. Y. N. Belokon, *Izv. Acad. Nauk, Ser. Khim.*, 1992, 1106; *Bull. Russ. Acad. Sci., Div. Chem. Sci.*, 1992, **41**, 868 (Engl. Trans.); and references therein; Y. N. Belokon, *Pure Appl. Chem.* 1992, **64**, 191; V. A. Soloshonok, D. V. Avilov, V. P. Kukhar, V. I. Tararov, T. F. Saveleva, T. D. Churkina, N. S. Ikonnikov, K. A. Kochetkov, S. A. Orlova, A. P. Pisarevsky, Y. T. Struchkov, N. I. Raevsky and Y. N. Belokon, *Tetrahedron: Asymmetry*, 1995, **6**, 1741; B. B. De and N. R. Thomas, *Tetrahedron: Asymmetry*, 1997, **8**, 2687; Y. N. Belokon, V. I. Tararov, V. I. Maleev, T. F. Saveleva and M. G. Ryzhov, *Tetrahedron: Asymmetry*, 1998, **9**, 4249; S. Collet, P. Bauchat, D. Danion – Bougot and R. Danion R, *Tetrahedron: Asymmetry*, 1998, **9**, 2121; V. A. Soloshonok, C. Z. Cai and V. J. Hruby, *Tetrahedron*, 1999, **55**, 12045; X. Tang, V. A. Soloshonok and V. J. Hruby V. J.: *Tetrahedron: Asymmetry*, 2000, **11**, 2917; C. Cai, V. A. Soloshonok and V. J. Hruby, *J. Org. Chem.*, 2001, **66**, 1339; Y. N. Belokon, K. A. Kochetkov, N. S. Ikonnikov, T. V. Strelkova, S. R. Harutyunyan and A. S. Saghiyan, *Tetrahedron: Asymmetry*, 2001, **12**, 481; A. Debache, S. Collet, P. Bauchat, D. Danion, L. Euzenat, A. Hercouet and B. Carboni, *Tetrahedron: Asymmetry*, 2001, **12**, 761; A. Popkov, A. Gee, M. Nádvorník and A. Lyčka, *Transition Metal Chem.*, 2002, **27**, 884; O. V. Larionov, T. F. Saveleva, K. A. Kochetkov, N. S. Ikonnokov, S. I. Kozhushkov, D. S. Yufit, J. A. K. Howard, V. N. Khrustalev, Y. N. Belokon and A. de Meijere, *Eur. J. Org. Chem.*, 2003, 869; Y. N. Belokon, K. A. Kochetkov and D. A. Borkin, *Mendeleev Commun.*, 2003, 132; H. Ueki, T. K. Ellis, C. H. Martin, T. U. Boettiger, S. B. Bolene and V. A. Soloshonok, *J. Org. Chem.*, 2003, **68**, 7104; A. S. Saghiyan, A. V. Geolchanyan, S. G. Petrosyan, T. V. Ghochikyan, V. S. Haroutunyan, A. A. Avetisyan, Y. N. Belokon and K. Fischer, *Tetrahedron: Asymmetry*, 2004, **15**, 705; X. Y. Gu, J. A. Ndungu, W. Qiu, J. F. Ying, M. D. Carducci, H. Wooden and V. J. Hruby, *Tetrahedron*, 2004, **60**, 8233; S. Vadon-Legoff, S. Dijols, D. Mansky and J.-L. Boucher, *Org. Process Res. & Develop.*, 2005, **9**, 677; V. A. Soloshonok, C. Cai, T. Yamada, H. Ueki, Y. Ohfune and V. J. Hruby, *J. Am. Chem. Soc.*, 2005, **127**, 15296; J.

C. Pessoa, I. Correia, A. Galvão, A. Gameiro, V. Felix and E. Fiuza, *J. Chem. Soc., Dalton Trans.*, 2005, 2312; A. Popkov, I. Císařová, J. Sopková, J. Jirman, A. Lyčka and K. A. Kochetkov, *Collect. Czech. Chem. Commun.*, 2005, **70**, 1397; A. S. Saghiyan, H. H. Hambardzumyan, L. L. Manasyan, A. A. Petrosyan, V. I. Maleev and A. S. Peregudov, *Synth. Commun.*, 2005, **35**, 449; A. S. Saghiyan, S. A. Dadayan, S. G. Petrosyan, L. L. Manasyan, A. V. Geolchanyan, S. M. Djamgaryan, S. A. Andreasyan, V. I. Maleev and V. N. Khrustalev, *Tetrahedron: Asymmetry*, 2006, **17**, 455. Application of the complexes for preparation of helically chiral precursors of nanostructures: V. A. Soloshonok and H. Ueki, *J. Am. Chem. Soc.* 2007, **129**, 2426.

3. Y. N. Belokon, DSc. Thesis, A. N. Nesmeyanov Institute of Organoelement Compounds, Acad. Sci. USSR 1979.
4. Y. N. Belokon, V. I. Tararov, V. I. Maleev, T. F. Saveleva and M. G. Ryzhov, *Tetrahedron: Asymmetry*, 1998, **9**, 4249.
5. V. I. Tararov, R. Kadyrov, C. Fischer and A. Börner, *Synlett*, 2004, 1961.
6. M. Nádvorník and A. Popkov, *Green Chem.*, 2002, 78.
7. Popkov, M. Nádvorník, P. Kružberská, A. Lyčka, M. Eisenhut, N. M. Gillings, *J. Labelled Compd. Radiopharm.*, 2003, **46**, S227; A. Popkov, M. Nádvorník, P. Kružberská, A. Lyčka, S. Lehel and N. M. Gillings, *J. Labelled Compd. Radiopharm.*, 2007, **50**, 370; M. S. Judenhofer, H. F. Wehrl, D. F. Newport, C. Catana, S. B. Siegel, M. Becker, A. Thielscher, M. Kneilling, M. P. Lichy, M. Eichner, K. Klingel, G. Reischl, S. Widmaier, M. Röcken, R. E. Nutt, H.-J. Machulla, K. Uludag, S. R. Cherry, C. D. Claussen and B. J. Pichler, *Nature Medicine* doi:10.1038/nm1700.
8. Y. N. Belokon, V. I. Bakhmutov, N. I. Chernoglazova, K. A. Kochetkov, S. V. Vitt, N. S. Garbalinskaya, and V. M. Belikov, *J. Chem. Soc., Perkin Trans. 1*, 1988, 305. For review, see: C. Cativiela and M. D. Días-de-Villegas, *Tetrahedron: Asymmetry*, 1998, **9**, 3517; C. Cativiela and M. D. Días-de-Villegas, *Tetrahedron: Asymmetry*, 2000, **11**, 645; H. Vogt and S Bräse, *Org. Biomol. Chem.*, 2007, **5**, 406; C. Najera, J. M. Sansano, *Chem. Rev.*, 2007, **107**, 4584; C. Cativiela, D. Días-de-Villegas, *Tetrahedron: Asymmetry* 2007, **18**, 569.
9. H. Franzen, L. Grehn and U. J. Ragnarsson, *J. Chem. Soc., Chem. Commun*., 1984, 1699.
10. *SMART and SAINT*: *Area Detector Control and Integration Software*, Bruker AXS Inc., Madison, WI, USA, 2003.
11. *SADABS*: Sheldrick G.M., *Program for Empirical Absorption Correction for Area Detectors (Version 2.10)*, University of Göttingen, Germany, 2003.
12. *SHELXTL*: *Structure Determination Programs (Version 6.12)*, Bruker AXS Inc., Madison, WI, USA, 2001.
13. *DIAMOND*: Brandenburg K., *Crystal and Molecular Structure Visualization (Version 3.1d)*, Crystal Impact GbR, Bonn, Germany, 2006.
14. P. Řehulka, A. Popkov, M. Nádvorník, J. Planeta, K. Mazanec, J. Chmelík, *J. Mass Spectrom*. 2006, **41**, 448.

Chapter 4.3

Off-line combination of reversed-phase liquid chromatography and laser desorption/ionization time-of-flight mass spectrometry with seamless post-source decay fragment ion analysis for characterization of squire-planar nickel(II) complexes

Pavel Řehulka[1], Alexander Popkov[2], Milan Nádvorník[3], Josef Planeta[1], Karel Mazanec[1] and Josef Chmelík[1]

[1]Institute of Analytical Chemistry, Brno, Czech Republic, [2]Faculty of Health and Social Studies, University of South Bohemia, České Budějovice, Czech Republic, [3]Department of General and Inorganic Chemistry, University of Pardubice, Czech Republic

J. Mass Spectrom. **2006**, *41*, 448

Abstract
Characterization of square-planar nickel(II) complexes of Schiff base of (*S*)-*N*-benzylproline (2-benzoylphenyl)amide and various amino acids that are used as efficient α-amino acids synthons was done using laser desorption/ionization time-of-flight mass spectrometry in off-line combination with liquid chromatography. A mixture of four square-planar nickel(II) complexes was separated using reversed-phase liquid chromatography and the separated fractions from the chromatographic run were directly from the column outlet spotted on the metal target using a lab-made sample deposition device. The separated fractions were then analyzed by laser desorption/ionization time-of-flight mass spectrometry. Seamless post-source decay fragment ion analysis was used for their structural characterization, which made possible the confirmation of expected chemical structures of analyzed compounds. The used off-line combination of separation by reversed-phase liquid chromatography and analysis by laser desorption/ionization time-of-flight mass spectrometry allowed successful separation, sensitive detection of square-planar nickel(II) complexes and elucidation of their structures.

Keywords
square-planar nickel(II) complexes, RP LC, LDI-TOF MS, off-line combination, seamless post-source decay.

Introduction
Mass spectrometry is often used as an efficient tool for confirmation or elucidation of the structure of organometallic compounds[1]. Matrix-assisted laser desorption/ionization[2], is usually not applicable for analysis of low molecular compounds due to the presence of matrix-related ions in the mass spectrum[3,4]. In some cases of analysis of small organic compounds, a special type of matrix can be used[5] or laser desorption/ionization (LDI) technique can be applied instead[6,7].
Usually, a target compound of the organic synthesis is present in a mixture with various impurities and by-products. The disadvantages of mass spectrometric analysis of such compound mixtures are ion suppression during ionization process and overlapping of signals in mass spectra[8,9]. The use of a suitable separation technique prior to mass spectrometry analysis often leads to an efficient solution of these problems[9,10]. Mass spectrometric techniques used for characterization of nonvolatile compounds can be combined with various chromatographic techniques, *e.g.* supercritical fluid chromatography (SFC)[11,12], size exclusion chromatography (SEC)[13,14], however, most frequently with high performance liquid chromatography (HPLC)[15].
This study focuses to the analysis of square-planar nickel(II) complexes of a common formula (Fig. 1) that were introduced by Belokon *et al.* as efficient α-amino acids synthons[16]. Several preparative procedures were developed for asymmetric synthesis of various amino acids starting from the complexes derived from glycine or racemic α-alanine[17]. Recent development towards environmentally friendly preparation and application of the complexes made them reagents of choice for multikilogram-scale synthesis of non-coded or labeled enantiomerically pure amino acids[18,19,20,21]. Complexes application for quick asymmetric synthesis of highly radioactive ^{11}C- or ^{18}F-labeled amino acids for positron emission tomography (PET) is now the most intensively studied field[22,23]. Industrial and biomedical applications require convenient and powerful analytical methods for both structure determination and quick analysis of a reaction mixture composition. While NMR[21,24,25], X-ray studies[21,25,26,27] and circular dichroism (CD)[21] studies of a number of such complexes were published, little information about mass spectral properties of the complexes is available. The only example of successful application of

^{252}Cf plasma-desorption mass spectrometry of negative ions for characterization of a thermally labile complex (Fig. 4.3.1, R=H, R'=Br) was published[24].

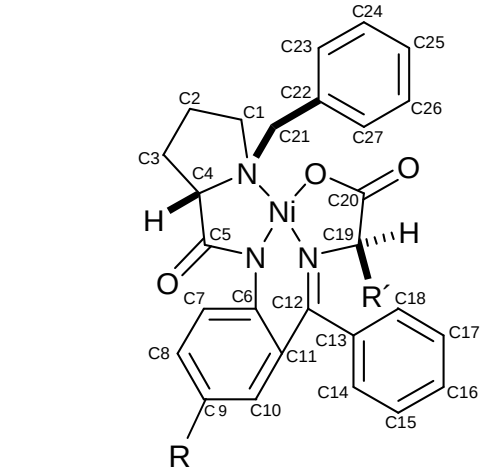

	GlyK	GlyK(Cl)	MetK	TyrK
Monoisotopic mass M	497.12	531.09	571.14	617.18
R	H	Cl	H	H
R´	H	H	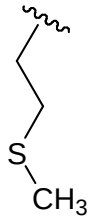	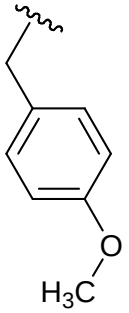

Figure 4.3.1 Chemical structure of analyzed nickel(II) complexes GlyK, GlyK(Cl), MetK, TyrK and their summary formulae with monoisotopic molecular masses.

This work shows the advantages of an off-line combination of reversed-phase liquid chromatography (RPLC) and laser desorption/ionization time-of-flight mass spectrometry (LDI-TOF MS) for characterization of organometallic compounds.

Experimental

Synthesis and characterization of nickel(II) complexes

A mixture of four nickel(II) complexes was used for the analysis. Their structures with monoisotopic molecular masses are shown in Fig. 4.3.1. Syntheses of a nickel(II) complex of the Schiff base of (*S*)-*N*-benzylproline (2-benzoylphenyl)amide and glycine ([N-[phenyl[2-[[[(1R,2S)-1-(phenylmethyl)-2-pyrrolidinyl-κN]carbonyl]-amino-κN]phenyl]-methylene]glycinato(2-)-κN,κO]nickel(II); GlyK), a nickel(II) complex of the Schiff base of (*S*)-*N*-benzylproline (2-benzoyl-4-chlorophenyl)amide and glycine ([N-[phenyl[5-chloro-2-[[[(1R,2S)-1-(phenylmethyl)-2-pyrrolidinyl-κN]-carbonyl]amino-κN]-phenyl]-methylene]glycinato(2-)-κN,κO]nickel(II); GlyK(Cl)) and a nickel(II) complex of the Schiff base of (*S*)-*N*-benzylproline (2-benzoylphenyl)amide and methionine ([N-[phenyl[2-

[[[(1R,2S)-1-(phenylmethyl)-2-pyrrolidinyl-κN]carbonyl]amino-κN]phenyl]-methylene]methioninato(2-)-κN,κO]nickel(II); MetK) are described elsewhere (GlyK[20], GlyK(Cl)[24], MetK[27]).

Synthesis of a nickel(II) complex of the Schiff base of (*S*)-*N*-benzylproline (2-benzoylphenyl)amide and (*S*)-2-amino-3-(4-methoxyphenyl)propanoic acid ([N-[phenyl[2-[[[(1R,2S)-1-(phenylmethyl)-2-pyrrolidinyl-κN]carbonyl]amino-kN]-phenyl]methylene]-4-methoxyphenylalaninato(2-)-κN,κO]nickel(II); TyrK) was carried out in a following way. Under argon atmosphere 2.5 M MeONa/MeOH (40 ml, 100 mmol) was added to a stirred suspension of (*S*)-*N*-benzylproline (2-benzoylphenyl)amide (1.54 g, 4.0 mmol)[18,19], *O*-methyl-L-tyrosine (4-methoxy-L-phenylalanine, (*S*)-2-amino-3-(4-methoxyphenyl)propanoic acid) (975 mg, 5.0 mmol) and $Ni(NO_3)_2 \cdot 6NH_3$ (1.85 g, 6.5 mmol) in dry MeOH (20 ml) at 50–55 °C. After stirring at 55 °C for 90 min, the mixture was poured into 10% aqueous citric acid (300 ml), stirred and the resulting precipitate was filtered off and dried in air. The dry precipitate was purified by column chromatography using silica gel (Merck 40/63) eluted with chloroform. The second red fraction, containing mixture of diastereomers of TyrK was collected. Yield was 1.68 g (68%). An analytical sample was purified by preparative TLC using silica gel (Merck 60H) eluted with CH_2Cl_2. The second red fraction, containing (*S*,*S*)–TyrK was collected. The obtained complex was then purified by chromatography on Sephadex LH-20 with toluene: MeOH = 2:1. M.p. 214–217 °C (from acetone). ^{1}H NMR (360.13 MHz, $CDCl_3$): 8.22 (d, 1H), 8.01 (d, 2H), 7.54 (m, 2H), 7.44 (t, 1H), 7.29 (m, 3H), 7.15 (m, 4H), 6.94 (d, 2H), 6.87 (d, 1H), 6.66 (d, 2H), 4.29 (d, 1H) and 3.46 (d, 1H) (AB system of $-CH_2Ar$, ^2J(H, H) = 12.7 Hz), 4.24 (A part of AMX system, dd, 1H), 3.03 (M part of AMX system, dd, 1H), 2.79 (X part of AMX system, dd, 1H), 3.82 (s, 3H, OCH_3), proline protons: 3.31 (m, 1H), 3.12 (m, 1H), 2.33 (m, 3H), 1.96 (m, 1H), 1.68 (m, 1H). For $C_{35}H_{33}N_3O_4Ni$ (average molecular mass: 618.34) calculated C 67.98%, H 5.38%, N 6.80%; found C 67.22%, H 5.77%, N 6.32%.

NMR spectroscopy was done with Bruker AMX 360 instrument. Temperature was 23 °C, hexamethyldisiloxane ($\delta(^1H)$=0.05 ppm) was used as internal standard. *Ab initio* calculation was performed using standard PC GAMESS program package[28,29].

Chromatographic separation

All four nickel(II) complexes were dissolved in acetonitrile to a concentration 10^{-3} M. The micro HPLC device consisted of a piston micropump MHPP20 (Laboratory Instruments, Prague, Czech Republic) and electrically driven Valco E90-220 sampling valve with a 200 nl internal sample loop. Separation was carried out on a home-made capillary RPLC column (length 250 mm, i.d. 320 μm)[30] filled with Biospher C18E (5 μm) particles (Labio Ltd., Prague, Czech Republic) and separated using mobile phase containing acetonitrile:water (3:1; v/v). Detection was performed in the flow cell, made from fused silica capillary i.d. 85 μm at wavelength 254 nm (Spectra 100, Thermo Separation Products, Florida, USA) together with chromatography station software CSW 1.7 (DataApex, Prague, Czech Republic) for signal evaluation. Sample injecting volume was 200 nl (this corresponds to 200 pmol of each species loaded onto the column) and the flow rate was approximately 4 μl min^{-1}. For an off-line combination of the RPLC separation and LDI-TOF MS analysis, a sample deposition device originally constructed for an off-line combination of supercritical fluid chromatography and matrix-assisted laser desorption/ionization time-of-flight mass spectrometry was used[31]. 10 sec fractions from the LC run were collected from the time 4:00 min to the time 7:10 on the metal target used for LDI-TOF MS analysis.

Mass spectrometry

LDI-TOF MS analysis was performed with the Kompact MALDI SEQ instrument (Shimadzu Biotech Kratos Analytical, Manchester, UK) in both linear and reflectron positive ionization mode. A nitrogen laser (λ=337 nm, 3 ns pulse width) and the curved field reflectron were used. The accelerating voltage was 20 kV and the measurements were performed using molecular mass-optimized delayed extraction. For a seamless post-source decay (sPSD) experiment, the width of the precursor ion selection using an ion gate was typically ±10 Th. Each positive ion LDI mass spectrum obtained was the sum of 25 unselected laser pulses on one sample preparation across the whole sample well. sPSD spectra were the sums of up to 250 laser pulses. All LDI mass spectra were smoothed using the company-supplied Savitsky-Golay algorithm and calibrated externally.

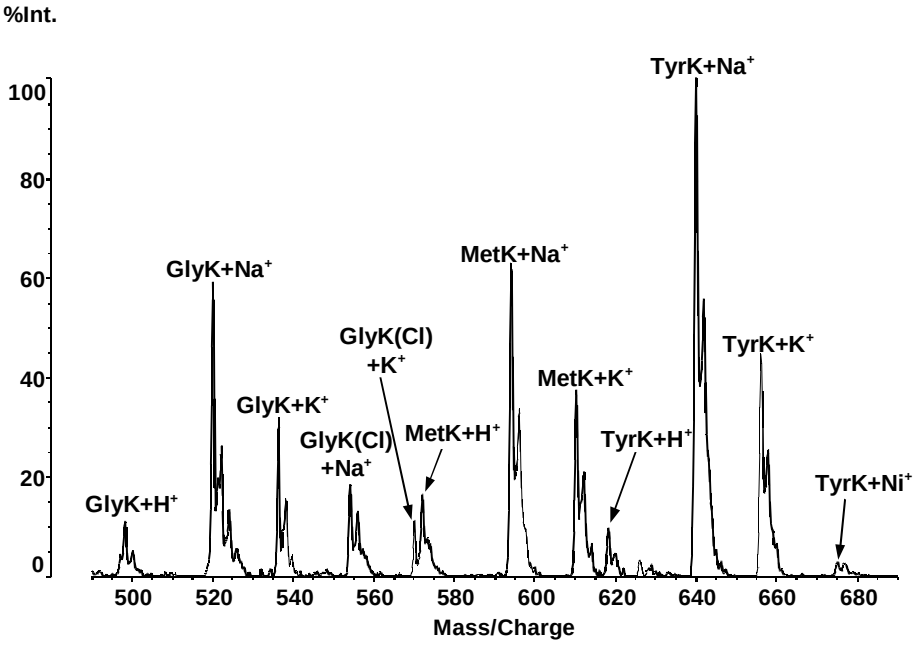

Figure 4.3.2 LDI-TOF MS measurement of unseparated mixture of four nickel(II) complexes GlyK, GlyK(Cl), MetK and TyrK.

Results and discussion

An LDI-TOF MS spectrum of unseparated equimolar (10^{-3} M per each component) mixture of four nickel(II) complexes is shown in Fig. 4.3.2. The spectrum is dominated by sodiated and potassiated species due to the presence of high amount of salts. In the case of GlyK(Cl) complex, its protonated form could not be detected, which was caused by ion suppression of other complexes present in the mixture resulting in overall decreased limit of detection.

Using the same sample as in the previous case, an sPSD experiment of each nickel(II) complex was carried out. Masses of protonated species were set as the values for precursor ion isolation since protonated species provided more structural information in comparison to sodiated and potassiated species. All sPSD spectra showed out low number of fragment ions with low signal-to-noise ratio (data not shown). Moreover, in the case of sPSD analysis of GlyK(Cl)

complex, the fragmentation comes from sodiated complex GlyK instead of protonated GlyK(Cl) complex, because the corresponding masses of both species are close and the ion gate is not able to separate them. Similar situation is in the case of complex MetK, resp. TyrK, where simultaneous fragmentation of $[GlyK(Cl)+Na]^+$ and $[MetK+H]^+$, resp. $[MetK+Na]^+$ and $[TyrK+H]^+$ occurred.

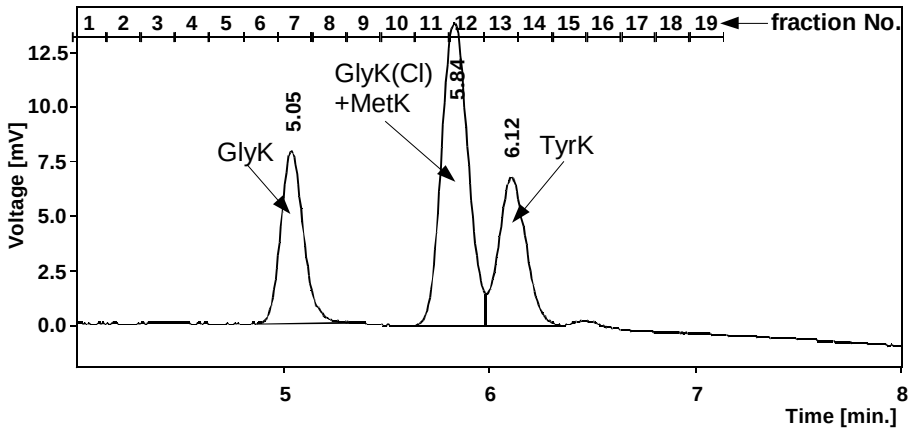

Figure 4.3.3 A chromatographic record of RPLC separation of nickel(II) complexes GlyK, GlyK(Cl), MetK and TyrK. The numbers above describe the fractions collected on the metal target using sample deposition device.

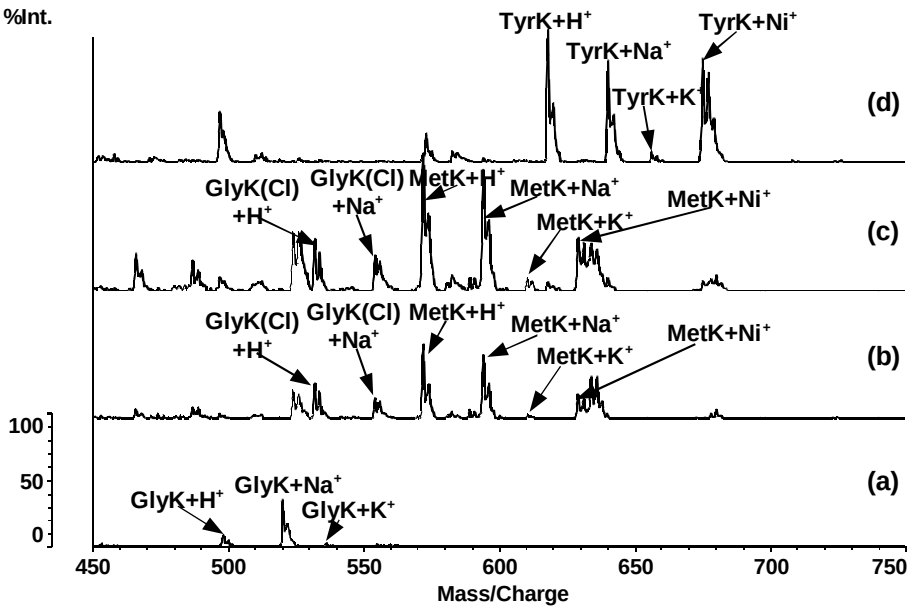

Figure 4 LDI-TOF MS analysis of fractions (a) 7, (b) 11, (c) 12, and (d) 13 from the RPLC separation of nickel(II) complexes GlyK, GlyK(Cl), MetK and TyrK.

The mixture of four nickel(II) complexes mixture was separated by capillary RPLC. The chromatogram showed good separation with the exception of overlapping peaks of GlyK(Cl) and MetK complexes (see Fig. 4.3.3). Identification of the peaks in the chromatogram was based on subsequent LDI-TOF MS analysis of the fractions deposited in 10 sec intervals on the target plate (for LDI-TOF MS analysis) using lab-made sample deposition device[31]. MS spectra of the fractions 7, 11, 12, and 13 are shown in Fig. 4.3.4. The complex GlyK was present in the fraction 7, the complexes GlyK(Cl) and MetK in the fractions 11 and 12, and the complex TyrK mainly in the fraction 13 and partially in the fraction 14.
sPSD analyses of these separated nickel(II) complexes are shown in Fig. 4.3.5. The RPLC separation of the mixture of nickel(II) complexes clearly improved the quality of the fragmentation spectra due to removal of salts and other compounds and the analyte decreased peak overlapping, thus the ion formation of a particular species was less suppressed by the presence of other species. The only exception was the analysis of GlyK(Cl) complex, where the presence of the in-source decay product of MetK complex was close to the protonated GlyK(Cl) complex, which complicates the interpretation of corresponding product ion spectra (Fig. 4.3.5b). However, the separation made possible the detection of protonated GlyK(Cl) complex and some of the product ions could be assigned to the fragments arising from this complex. The identifications of fragment ions present in sPSD spectra are shown in the insets in Fig. 4.3.5. The expected chemical structure of particular nickel(II) complexes was successfully confirmed in this way.

	Singlet		Triplet	
	Energy, Hartree		Energy, Hartree	
RHF/ROHF	-1985.7830		-1985.8472	
MP2	-1987.7208		-1987.7110	
	Bond order	Bond length, nm	Bond order	Bond length, nm
Ni-N	0.490	0.1894	0.249	0.2155
Ni-C4	0.897	0.1869	<0.050	0.2726
Ni-C22	0.052	0.2618	0.067	0.2562
Ni-C23	0.128	0.2546	0.105	0.2497
	MP2 Mulliken charge		MP2 Mulliken charge	
Ni	0.822		0.730	
N	-0.265		-0.302	
C4	-0.326		-0.109	
C22	0.150		0.126	
C23	-0.390		-0.357	

Table 4.3.1 Calculated structural features of the positive ion 217.

Among all fragments, the ion 217 Da attracted our attention. It corresponds to a nickel atom coordinated to *N*-benzylpyrroline. While not very intensive in LDI mass spectra, this ion is usually one of the most intensive fragment ions in EI, FAB and ^{252}Cf plasma-desorption (PD) mass spectra[32]. We performed *ab initio* calculations in order to disclose its structure. Initial atom coordinates for structure optimization were derived from X-ray data for GlyK[25] by breaking C4-C5, Ni-N, Ni-N_α and Ni-O bonds (Fig. 4.3.1). Due to computational limitations,

two independent structure optimizations for singlet and triplet states of the positive ion were performed at RHF/ROHF level (TZV(d) basis set for C and N; TZV basis set for Ni and H)[33,34] using PC GAMESS program package[28,29]. Electronic structure data are evaluated in terms of Mulliken population analysis. During optimization the aromatic ring approached the nickel atom in both cases. Optimized N-C21-C22 angles (110.7^{o} for triplet and 109.0^{o} for singlet states, respectively) are close to the optimal angle for sp^3 hybridization of carbon atom. For the resulting structures MP2 single-point calculations in the same basis set show that the energy difference between both states is negligible, only 26 kJ mol^{-1} (Table 4.3.1). Similar energies of these two states indicate a spin-contaminated state of a real ion. Thus a time-consuming CI approach should be used in future for correct modeling of geometry. Both calculated structures own common features: negative charges on C23 and the nitrogen atom are responsible for stabilization of the molecule – both *N*-pyrroline part and aromatic part of the ligand are bonded to the nickel atom.

According to the theoretical computation, the fragment ion of mass value 217 Da should appear in LDI mass spectra. While this ion was present in a smaller amount in the MS spectra of the fractions 7, 11, 12 and 13, corresponding sPSD analysis of the same fractions showed this fragment only in the case of GlyK(Cl) complex. However, in all cases abundant peaks at m/z 160 were present that are formed as either decay products of the fragment ion 217 or directly from the protonated parent molecules. Beside the fragment ion 160, in all cases the complementary fragment ions were observed (GlyK: 338, GlyK(Cl): 372, MetK: 412, TyrK: 458). Moreover, these complementary ions showed neutral loss of CO (-28) well seen in the cases of GlyK and GlyK(Cl) and with low intensity for MetK.

All four complexes showed the loss of HCO_2. Only in the case of MetK the corresponding peak is overlapped with the fragment ion 524. Similar loss was observed with all previously studied analogous complexes in both positive and negative ions EI, FAB and ^{252}Cf plasma-desorption mass spectra[32]. For MetK and TyrK, the intensive losses of amino acid side chains are observed. While in the case of TyrK the side chain is lost in one step (m/z 497), MetK looses its side chain in two ways: partly (–SCH_3, m/z 524) and completely (–$CH_2CH_2SCH_3$, m/z 497). For MetK the first pathway could be preferred due to formation of stable complex of 2-aminobuten-2-oic acid[27], the second pathway – due to stabilization of $CH_2CH_2SCH_3$ fragment by formation of a cyclic product.

The off-line combination of RPLC and LDI-TOF MS is a useful tool for improvement of detection limit for nickel(II) complexes present in mixtures. The RPLC separation preceding MS analysis also enables confirmation of the compound identity using sPSD analysis, which is not possible in the original mixture. An alternative method based on on-line combination of RPLC separation and ESI-MS^n analysis will be studied in near future with the aims of both structure elucidation and comparison of fragmentation pathways with LDI-TOF MS (LDI pathway was different to those observed in EI, FAB and PD).

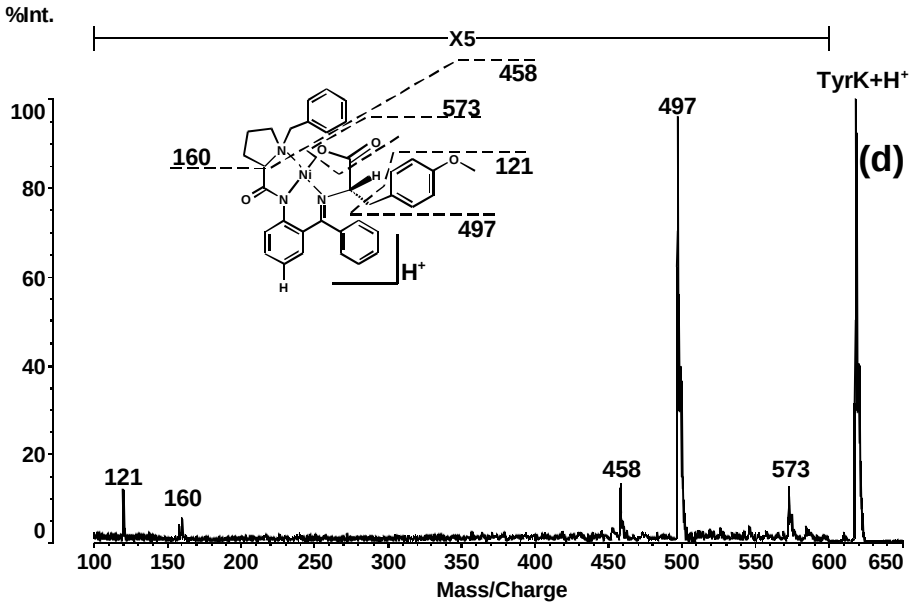
%Int.
X5
458
573
160
121
497
H+
TyrK+H+
497
(d)
121
160
458
573
100
80
60
40
20
0
100 150 200 250 300 350 400 450 500 550 600 650
Mass/Charge

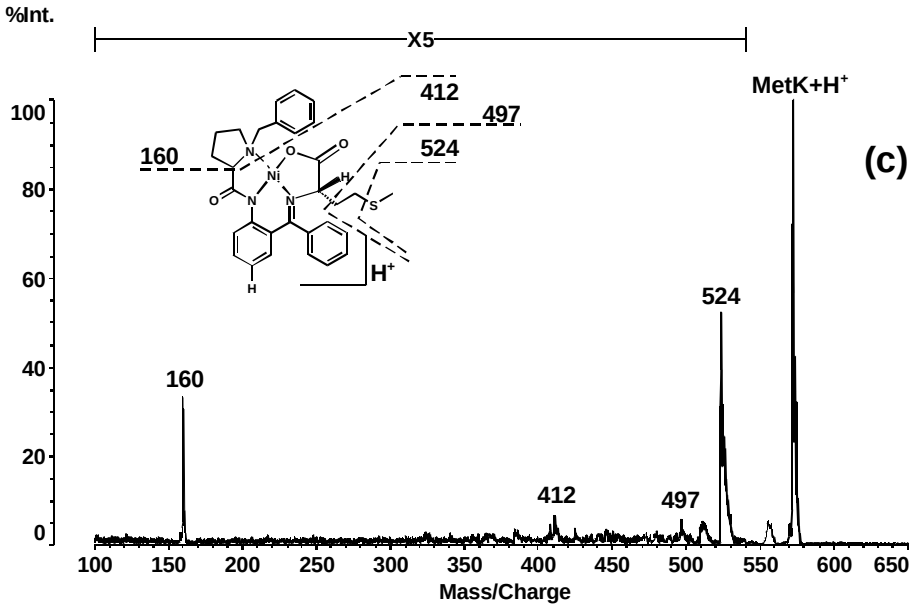
%Int.
X5
412
497
524
160
H+
MetK+H+
(c)
524
160
412
497
100
80
60
40
20
0
100 150 200 250 300 350 400 450 500 550 600 650
Mass/Charge

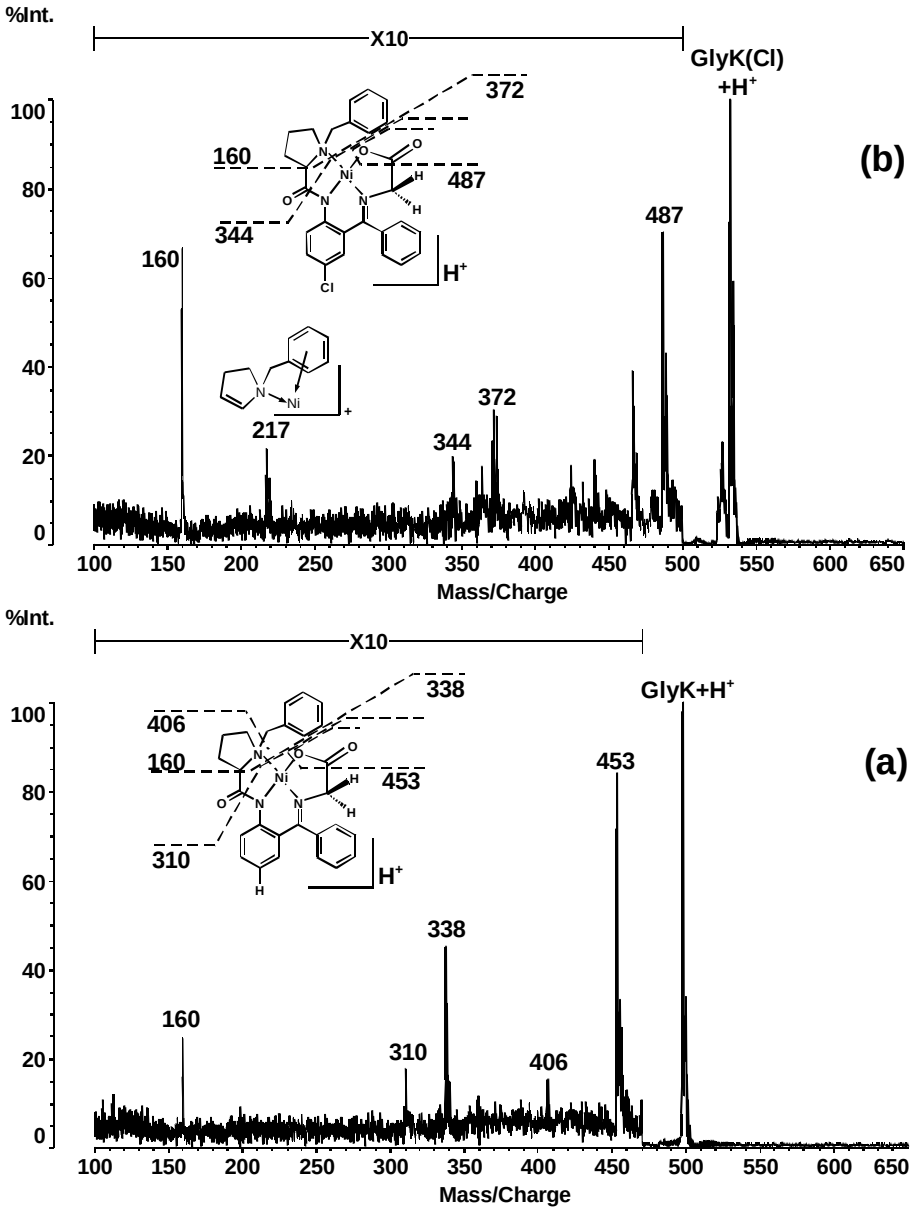

Figure 4.3.5 sPSD analysis of nickel(II) complexes after the RPLC separation. (a) – GlyK, (b) – GlyK(Cl), (c) – MetK and (d) – TyrK.

Acknowledgement

The authors thank Professor Antonín Lyčka for recording and interpretation of the proton NMR spectrum. This work was supported by a grant No. A4031104 from the Grant Agency of Academy of Sciences of the Czech Republic, a grant No. 203/05/2106 from the Grant Agency of the Czech Republic, a grant MSM 6007665808, and a grant Z40310501.

REFERENCES

1. Traeger JC. Electrospray mass spectrometry of organometallic compounds. *Int. J. Mass Spectrom.* 2000; **200**: 387. DOI: 10.1016/S1387-3806(00)00346-8.
2. Karas M, Hillenkamp F. Laser desorption ionization of proteins with molecular masses exceeding 10,000 daltons. *Anal. Chem*. 1988; **60**: 2299. DOI: 10.1021/ac00171a028.
3. Keller BO, Li L. Discerning matrix-cluster peaks in matrix-assisted laser desorption/ionization time-of-flight mass spectra of dilute peptide mixtures. *J. Am. Soc. Mass Spectrom.* 2000; **11**:88. DOI: 10.1016/S1044-0305(99)00126-9.
4. Řehulka P, Šalplachta J, Chmelík J. Improvement of quality of peptide mass spectra in matrix-assisted laser desorption/ionization time-of-flight mass spectrometry and post-source decay analysis of salty protein digests by using on-target washing. *J. Mass Spectrom.* 2003; **38**: 1267. DOI: 10.1002/jms.548.
5. Stubiger G, Pittenauer E, Allmaier G. Characterisation of castor oil by on-line and off-line non-aqueous reverse-phase high-performance liquid chromatography - mass spectrometry (APCI and UV/MALDI). *Phytochem. Anal.* 2003; **14**: 337. DOI: 10.1002/pca.724.
6. Ramsey BG, Bier ME. A laser desorption ionization mass spectrometry investigation of triarylboranes and tri-9-anthrylborane photolysis products. *J. Organomet. Chem.* 2005; **690**: 962. DOI: 10.1016/j.jorganchem.2004.11.002.
7. Chen R, Li L. Reactions of atomic transition-metal ions with long-chain alkanes. *J. Am. Soc. Mass Spectrom.* 2001; **12**: 367. DOI: 10.1016/S1044-0305(01)00217-3.
8. Burlingame AL, Medzihradszky KF, Clauser KR, Hall SC, Maltby DA, Walls FC. From protein primary sequence to the gamut of covalent modifications using mass spectrometry. *ACS Symposium Series*. 1996; **619**: 472.
9. Preisler J; Hu P, Rejtar T, Karger BL. Capillary electrophoresis-matrix-assisted laser desorption/ionization time-of-flight mass spectrometry using a vacuum deposition interface. *Anal. Chem.* 2000; **72**: 4785. DOI: 10.1021/ac0005870.
10. Murray KK. Coupling matrix-assisted laser desorption/ionization to liquid separations. *Mass Spectrom. Rev.* 1997; **16**: 283. DOI: 10.1002/(SICI)1098-2787(1997)16:5<283::AID-MAS3>3.0.CO;2-D.
11. Combs MT, Ashraf-Khorassani M, Taylor LT. Packed column supercritical fluid chromatography mass spectroscopy: A review. *J. Chromatogr. A.* 1997; **785**: 85. DOI: 10.1016/S0021-9673(97)00755-3.
12. Chmelík J, Planeta J, Řehulka P, Chmelík J. Determination of molecular mass distribution of silicone oils by supercritical fluid chromatography, matrix-assisted laser desorption ionization time-of-flight mass spectrometry and their off-line combination. *J. Mass Spectrom.* 2001; **36**: 760. DOI: 10.1002/jms.179.
13. Montaudo MS. Mass spectra of copolymers. *Mass Spectrom. Rev.* 2002; **21**: 108. DOI: 10.1002/mas.10021.
14. Šalplachta J, Řehulka P, Chmelík J. Identification of proteins by combination of size-exclusion chromatography with matrix-assisted laser desorption/ionization time-of-flight mass spectrometry and comparison of some desalting procedures for both intact proteins and their tryptic digests. *J. Mass Spectrom.* 2004; **39**: 1395. DOI: 10.1002/jms.700.

15. Lee H. Pharmaceutical applications of liquid chromatography coupled with mass spectrometry (LC/MS). *J. Liq. Chromatogr. Relat. Technol.* 2005; **28**: 1161. DOI: 10.1081/JLC-200053022.
16. Belokon YN, Bulychev AG, Vitt SV, Struchkov YT, Batsanov AS, Timofeeva TV, Tsyryapkin VA, Ryzhov MG, Lysova LA, Bakhmutov VI, Belikov VM. General method of diastereo- and enantio-selective synthesis of β-hydroxy-α-amino acids by condensation of aldehydes and ketones with glycine. *J. Am. Chem. Soc.* 1985; **107**: 4252. DOI: 10.1021/ja00300a030.
17. Belokon YN. Chiral complexes of Ni(II), Cu(II), and Cu(I) as reagents, catalysts and receptors for asymmetric synthesis and chiral recognition of amino acids. *Pure Appl. Chem.* 1992; **64**: 1917.
18. Belokon YN, Tararov VI, Maleev VI, Saveleva TF, Ryzhov MG. Improved procedures for the synthesis of (*S*)-2-[*N*-(*N* '-benzylprolyl)amino]benzophenone (BPB) and Ni(II) complexes of Schiff's bases derived from BPB and amino acids. *Tetrahedron: Asymmetry* 1998; **9**: 4249. DOI: 10.1016/S0957-4166(98)00449-2.
19. Tararov VI, Kadyrov R, Fischer C, Börner A. Selective *N*-benzylation of amino acids under homogeneously catalyzed hydrogenation conditions. *Synlett* 2004; 1961. DOI: 10.1055/s-2004-830855.
20. Nádvorník M, Popkov A. Improved synthesis of the Ni(II) complex of the Schiff base of (S)-2-[N-(N '-benzylprolyl)amino]benzophenone and glycine. *Green Chem.* 2002; **4**: 71. DOI: 10.1039/b109806c.
21. Popkov A, Císařová I, Sopková J, Jirman J, Lyčka A, Kochetkov KA. Asymmetric synthesis of (*S*)-2-amino-3-(1-naphthyl)propanoic acid *via* chiral nickel complex. Crystal structure, circular dichroism, ^{1}H NMR and ^{13}C NMR spectra of the complex. *Collect. Czech. Chem. Commun.* 2005; **70**: 1397. DOI: 10.1135/cccc20051397.
22. Fasth KJ, Långström B. Asymmetric synthesis of L-[beta-C-11]amino acids using a chiral nickel complex of the Schiff base of (*S*)-o-[(*N*-benzylprolyl)amino]benzophenone and glycine. *Acta Chem. Scand.* 1990; **44**: 720.
23. Krasikova RN, Kuznetsova OF, Fedorova OS, Mosevich IK, Maleev VI, Belokon YN. The application of stoichiometric asymmetric synthesis to the preparation of 2-[^{18}F]fluoro-L-alpha-methyl tyrosine, potential agent for PET imaging of tumors. *Eur. J. Nucl. Med. and Molecular Imaging*, 2004; **31**: S381.
24. Popkov A, Jirman J, Nádvorník M, Manorik PA. NMR study of the structures of Ni(II) complexes of Schiff bases of 2-bromoglycine with (*S*)-2-(*N*-benzylprolyl)aminobenzophenone or (*S*)-2-(*N*-benzylprolyl)amino-5-chlorobenzophenone. *Collect. Czech. Chem. Commun.* 1998; **63**: 990. DOI: 10.1135/cccc19980990.
25. Popkov A, Langer V, Manorik PA, Weidlich T. Long-range spin-spin interactions in ^{13}C-NMR spectra of the nickel(II) complex of Schiff base of (*S*)-*N*-benzylproline (2-benzoylphenyl)amide and glycine. Quantum-chemical calculations and possible donation of electron density from the π-system of the benzyl group to nickel. *Transition Metal Chem.* 2003; **28**: 475. DOI: 10.1023/A:1023691827124.
26. Kožíšek J, Fronc M, Skubák P, Popkov A, Breza M, Fuess H, Paulmann C. Electronic structure of the nickel(II) complex of Schiff base of (*S*)-*N*-benzylproline (2-benzoylphenyl)amide and glycine. *Acta Crystallogr. A*, 2004; **60**: 510. DOI: 10.1107/S0108767304017131.

27. Belokon YN, Sagyan AS, Djamgaryan SA, Bakhmutov VI, Vitt SV, Batsanov AS, Struchkov YT, Belikov VM. General method for the asymmetric synthesis of antidiastereoisomers of beta-substituted L-2-aminobutanoic acids via chiral nickel(II) Schiff base complexes of dehydroaminobutanoic acid – X-ray crystal and molecular structure of the nickel(II) complex of the Schiff base from (S)-2-[*N*-(benzylprolyl)amino]benzophenone and dehydroaminobutanoic acid. *J. Chem. Soc.-Perkin Trans. 1*. 1990; 2301. DOI: 10.1039/P19900002301.
28. GAMESS (US): Schmidt MW, Balridge KK, Boatz JA, Elbert ST, Gordon MS, Jensen JJ, Koseki S, Matsunaga N, Nguyen KA, Su S, Windus TL, Dupuis M, Montgomery JA. General atomic and molecular electronic structure system. *J. Comput. Chem.* 1993; **14**: 1347. DOI: 10.1002/jcc.540141112.
29. PC GAMESS: Granovsky AA. http://classic.chem.msu.su/gran/gamess/index.html
30. Planeta J, Karásek P, Vejrosta J. Development of packed capillary columns using carbon dioxide slurries. *J. Sep. Sci.* 2003; **26**: 525. DOI: 10.1002/jssc.200390071.
31. Planeta J, Řehulka P, Chmelík J. Sample deposition device for off-line combination of supercritical fluid chromatography and matrix-assisted laser desorption/ionization time-of-flight mass spectrometry. *Anal. Chem.* 2002; **74**: 3911. DOI: 10.1021/ac020085h.
32. Čermak J, Ubik K, Reztsová N, Chivanov V, Popkov A, unpublished results.
33. Dunning TH. Gaussian basis functions for use in molecular calculations. III. Contraction of (10s6p) atomic basis sets for the first-row atoms. *J. Chem. Phys.* 1971; **55**: 716. DOI: 10.1063/1.1676139.
34. Rappe AK, Smedley TA, Goddard WA. Flexible d basis sets for Sc through Cu. *J. Phys. Chem*. 1981; **85**, 2607. DOI: 10.1021/j150618a007.

Chapter 4.4

Characterization of Ni(II) Complexes of Schiff Bases of Amino Acids and (*S*)-*N*-(2-benzoylphenyl)-1-benzylpyrrolidine-2-carboxamide Using Ion Trap and QqTOF Electrospray Ionization Tandem Mass Spectrometry

Robert Jirásko[1], Michal Holčapek[1], Lenka Kolářová[1], Milan Nádvorník[2], Alexander Popkov[3]

[1]Department of Analytical Chemistry, [2]Department of General and Inorganic Chemistry, University of Pardubice, Czech Republic, [3] Department of Nuclear Medicine and Molecular Imaging, University Medical Center Groningen, University of Groningen, The Netherlands

J. Mass Spectrom., DOI: 10.1002/jms.1405

Abstract

This work demonstrates the application of electrospray ionization mass spectrometry (ESI-MS) using two different mass analyzers, ion trap and hybrid quadrupole time-of-flight mass analyzer (QqTOF), for the structural characterization of Ni(II) complexes of Schiff bases of (*S*)-*N*-(2-benzoylphenyl)-1-benzylpyrrolidine-2-carboxamide with different amino acids. ESI enables the molecular weight determination on the basis of rather simple positive-ion ESI mass spectra containing only protonated molecules and adducts with sodium or potassium ions. Fragmentation patterns are characterized by tandem mass spectrometric experiments, where both tandem mass analyzers provide complementary information. QqTOF data are used for the determination of elemental composition of individual ions due to mass accuracies always better than 3 ppm with the external calibration, while multistage tandem mass spectra obtained by the ion trap are suitable for studying the fragmentation paths. The novel aspect of our approach is the combination of mass accuracies and relative abundances of all isotopic peaks in isotopic clusters providing more powerful data for the structural characterization of organometallic compounds containing polyisotopic elements. The benefit of relative and absolute mean mass accuracies is demonstrated on the example of studied Ni(II) complexes.

Introduction

Ni(II) complexes of Schiff bases of (*S*)-*N*-(2-benzoylphenyl)-1-benzylpyrrolidine-2-carboxamide and different amino acids are being developed as artificial analogues of pyridoxal 5'-phosphate (PLP) dependent enzymes [1]. Their preparative applications for stoichiometric asymmetric synthesis of α-amino acids have been optimized by a number of groups worldwide [2-6]. These complexes are also precursors for helically chiral nanomaterials [7]. The scheme of their preparation is shown in Fig. 4.4.1. This reaction promotes mainly the formation of *S*,*S*-diastereomer due to thermodynamic control of stereochemistry of the newly created asymmetric center [8,9]. The preparation of peptide analogues stable towards proteases is a versatile approach in the development of peptidomimetic drug candidates. They can also be used as conformationally restricted models of natural peptides for nuclear magnetic resonance (NMR), circular dichroism and crystallographic investigations [11]. For positron emission tomography [10,11], β^+-emitting radiopharmaceuticals can be prepared by the introduction of labeled ^{11}C-methyl group by the reaction of particular complex of α-amino acid with labelled $^{11}CH_3I$ or by the alkylation with a ^{18}F-bearing benzylhalogenide. In case of amino acid containing nucleophilic heteroatoms in its side-chain, such as tryptophan (nitrogen) and tyrosine (oxygen), the methylation could take place on these heteroatoms instead of desired α-carbon of amino acid. Therefore, it is necessary to protect heteroatoms using a suitable protective group, *e.g. tert*-butyl or *tert*-butyl carbamate (Boc) protective groups. Chiral synthons of α-amino acids labeled with ^{13}C or ^{15}N are useful tools in the preparation of α-amino acids that are enantiomerically pure and selectively isotopically substituted for NMR and mass spectrometry (MS) studies of biological systems [12]. The established method used for the structure elucidation of organonickel compounds is NMR based on ^{1}H and ^{13}C chemical shifts [13,14]. When a single crystal can be prepared, then X-ray is a method of choice [9,15] due to the highest solid-state structural information content, but on the other hand the preparation of single crystal may be time-consuming or impossible in some cases.

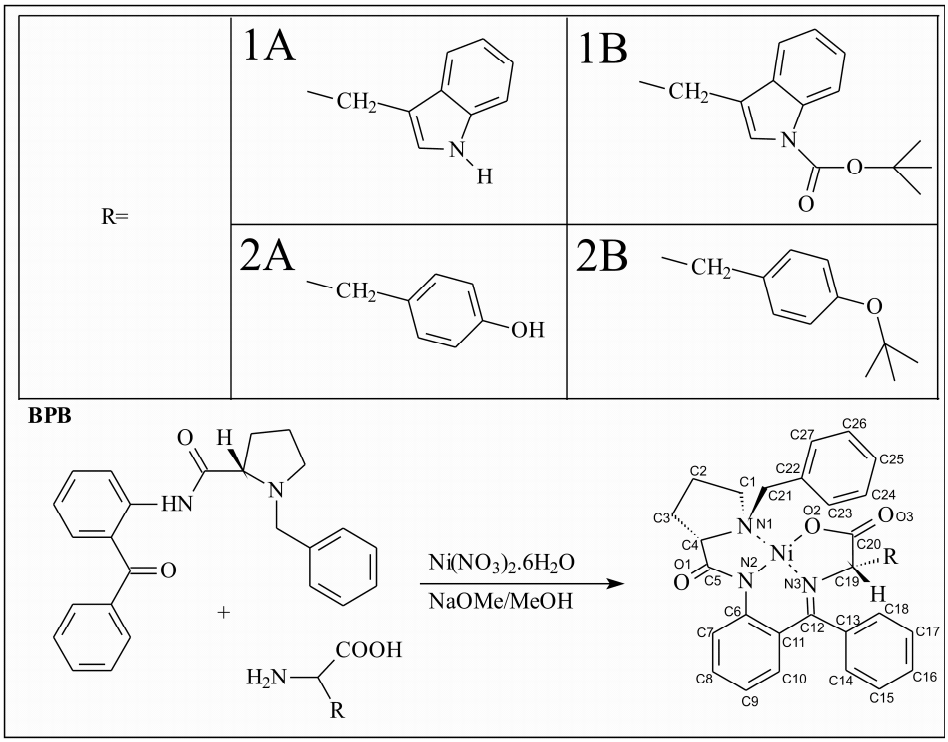

Figure 4.4.1 Structures of studied compounds and the reaction scheme of their preparation.

Electrospray ionization (ESI) is the most suitable ionization technique for the analysis of various metal complexes with amino acids and small peptides, for example Cu(II) [16, 17], Fe(II) [17] or Ni(II) [18] complexes can be used for differentiation of positional isomers (leucine vs. isoleucine) [16], diastereoisomers [17] and chiral isomers [18]. Studies of copper complexes have been published in numerous works [19-31], but this is the first work devoted exclusively to Ni(II) complexes of amino acids using ESI-MS. Only one previous work of similar Ni(II) was based on matrix-assisted laser desorption/ionization (MALDI), where the ionization and fragmentation behavior show some differences comparing to present work [32]. The ion trap analyzer is ideally suited for fragmentation pattern studies [17], while the benefit of time-of-flight (TOF) based mass analyzers [32] is mainly in the high-resolution and high mass accuracy applicable for the structure elucidation and reliable elemental composition determination. Based on our previous works dealing with the characterization of organotin compounds using ion trap ESI-MS [33-35], we have applied a combination of both ion trap and hybrid quadrupole time-of-flight mass analyzer (QqTOF) for the structure elucidation of amino acid nickel complexes providing complementary data. Moreover, the fragmentation behavior is compared with previous studies of Cu(II) complexes of amino acids to look for both similarities and differences.

Experimental part

Ni(II) complexes of Schiff bases of (*S*)-*N*-(2-benzoylphenyl)-1-pentamethylbenzylpyrrolidine-2-carboxamide and glycine or (^{15}N)glycine were prepared using a standard procedure previously described for similar complexes derived from non-pentamethylated (*S*)-*N*-(2-benzoylphenyl)-1-benzylpyrrolidine-2-carboxamide and glycine or (^{15}N)glycine [12]. The

compounds were fully characterized by ^{1}H-NMR, ^{13}C-NMR and tandem mass spectrometric techniques. Their structures and scheme of their preparation are shown in Fig. 4.4.1. The possible methylation products (explained in Results and discussion) are shown in Fig. 4.4.2. These compounds provided a signal only in the positive-ion ESI-MS mode and they were characterized using two different tandem mass spectrometers.

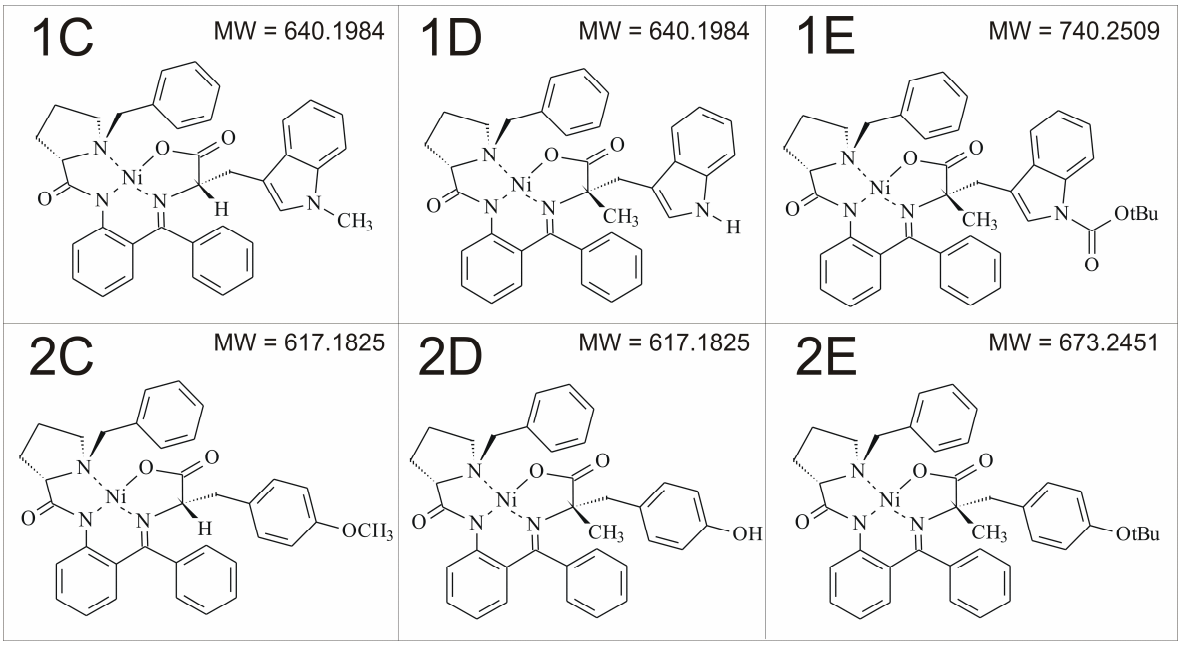

Figure 4.4.2 Possible structures of methylation products for protected tryptophan (**1**) and tyrosine (**2**) complexes.

1) Ion trap analyzer (Esquire 3000, Bruker Daltonics, Germany) - the mass spectra were measured in the range *m/z* 50 - 1000. The samples were dissolved in acetonitrile and analyzed by direct infusion at the flow rate of 5 μl/min. The ion source temperature was 300°C, the flow rate and the pressure of nitrogen were 4 l/min and 10 psi, respectively. The selected precursor ions were further analyzed by MS/MS analyses under the following conditions: the isolation width Δ*m/z* 6, the collision amplitude in the range 0.8 – 0.9 V depending on the precursor ion stability.
2) Hybrid QqTOF analyzer (micrOTOF-Q, Bruker Daltonics, Germany) – the mass spectra were measured in the range *m/z* 50 – 1000. The instrument was externally calibrated using ESI tuning mix before the individual measurements. The samples were dissolved in acetonitrile and analyzed by direct infusion at the flow rate of 3 μl/min. Interface parameters were set as follows: capillary voltage = -4.5 kV, drying temperature = 200°C, the flow rate and pressure of nitrogen were 4 l/min and 0.4 bar, respectively. Data were acquired by summation of 50000 scans with 10 rolling averages during two minutes to obtain the accurate masses. The collision energy for tandem mass spectra measurements was set in the range 25 eV/z – 30 eV/z.
For the confirmation of proposed fragmentation paths, other labeled complexes were synthesized and analyzed by MS/MS: ^{15}N3, ^{13}C19 and ^{13}C20. All measurements were repeated in perdeuterated methanol (CD_3OD) to obtain deuterated molecule $[M+D]^+$ for easier localization of protonation (deuteration) site. The same was also done with $[M+Na]^+$ ions.

Table 4.4.1 Theoretical masses, mass accuracy, relative mean mass accuracy, absolute mean mass accuracy and sigma value for deprotonated molecules, sodium and potassium molecular adducts for all studied compounds (values are in ppm except for sigma)

		$[M+H]^+$	$[M+Na]^+$	$[M+K]^+$
Compound **1A**	Theoretical *m/z*	627.1901	649.1720	665.1459
	Mass accuracy	-0.1	-0.4	-0.3
	Relative mean mass accuracy	-0.2	-0.3	-1.3
	Absolute mean mass accuracy	0.6	0.5	1.7
	Sigma	0.015	0.009	0.027
Compound **1B**	Theoretical *m/z*	727.2425	749.2244	765.1984
	Mass accuracy	2.6	2.4	0.9
	Relative mean mass accuracy	2.3	1.8	1.0
	Absolute mean mass accuracy	2.3	1.7	1.0
	Sigma	0.010	0.008	0.018
Compound **1C**	Theoretical *m/z*	641.2057	663.1877	679.1616
	Mass accuracy	-0.9	0.0	-3.2
	Relative mean mass accuracy	-1.0	0.5	-2.5
	Absolute mean mass accuracy	1.0	0.7	2.6
	Sigma	0.013	0.012	0.020
Compound **2A**	Theoretical *m/z*	604.1741	626.1560	642.1300
	Mass accuracy	-2.6	-1.1	-2.3
	Relative mean mass accuracy	-2.5	-1.8	-1.6
	Absolute mean mass accuracy	2.6	1.9	2.3
	Sigma	0.023	0.008	0.021
Compound **2B**	Theoretical *m/z*	660.2367	682.2186	698.1926
	Mass accuracy	0.4	1.2	0.6
	Relative mean mass accuracy	0.1	0.7	0.2
	Absolute mean mass accuracy	0.6	0.7	0.6
	Sigma	0.014	0.011	0.013
Compound **2E**	Theoretical *m/z*	674.2523	696.2343	712.2082
	Mass accuracy	-0.5	-0.7	0.2
	Relative mean mass accuracy	-0.5	7.2 [a]	-0.4
	Absolute mean mass accuracy	0.5	9.2 [a]	0.9
	Sigma	0.004	0.045 [a]	0.019

[a] Partial overlap with non-resolved [M+K]+ ion of **2B**.

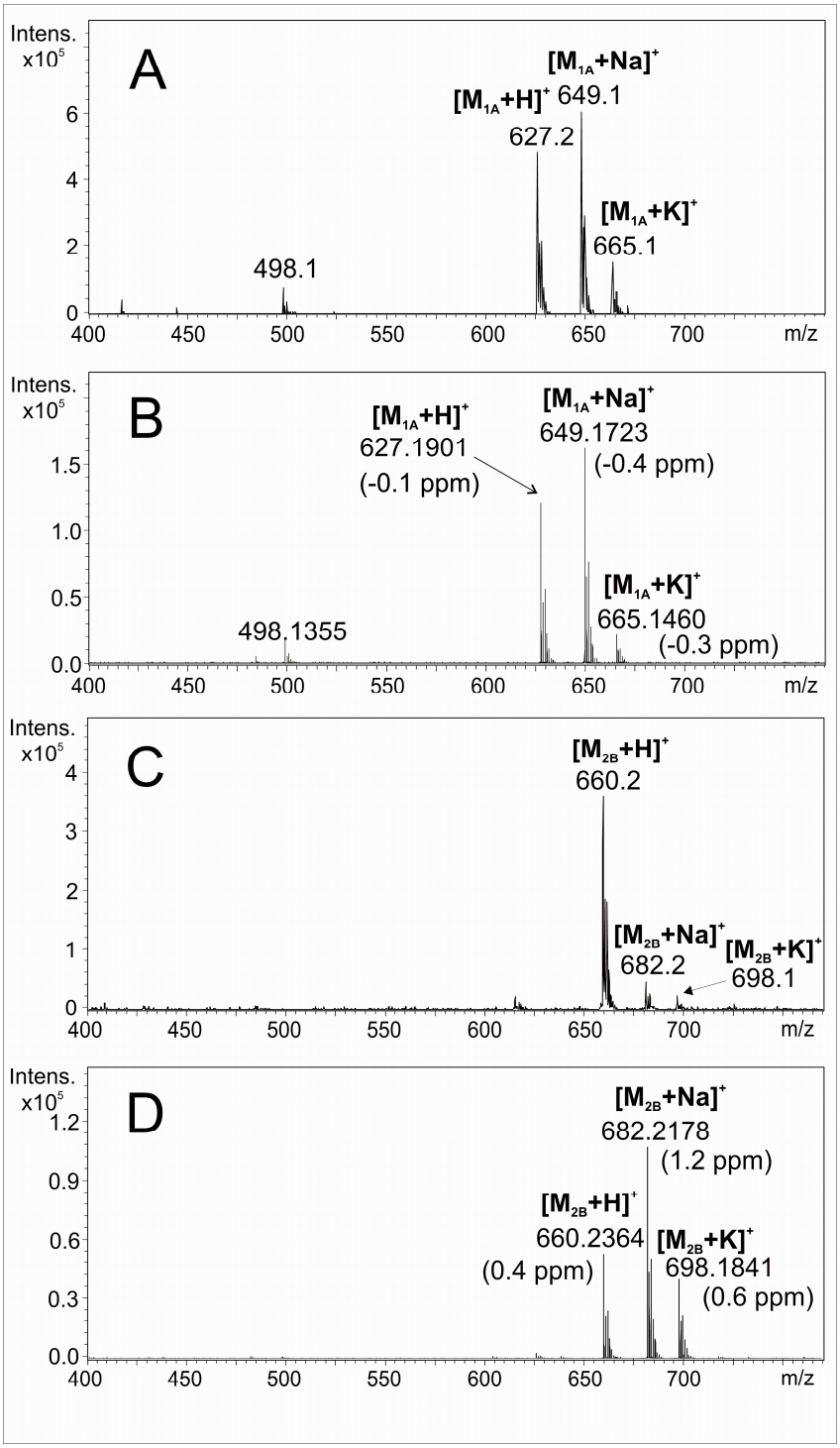

Figure 4.4.3 Full scan positive-ion ESI mass spectra: A/ ion trap spectrum of compound **1A**, B/ QqTOF spectrum of compound **1A**, C/ ion trap spectrum of compound **2B**, D/QqTOF spectrum of compound **2B**.

Results and discussion

Protonated molecules $[M+H]^+$ and adducts with alkali metal ions $[M+Na]^+$ and $[M+K]^+$ are observed in the full scan positive-ion ESI mass spectra for both analyzers (Fig. 4.4.3). The main difference between these spectra is the resolution and mass accuracy, both is much better for QqTOF analyzer (Table 4.4.1). The exact evaluation of experimental isotopic distribution and the comparison with theoretical data is a useful tool in the mass spectra interpretation of polyisotopic elements such as tin [34, 35], germanium [36], nickel and many others, because polyisotopic elements significantly contribute to the total isotopic distribution. This approach can reveal their presence or absence in the structure of individual ions. The comparison of theoretical and experimental isotopic distributions is shown in Fig. 4 on the example of $[M+H]^+$ ion for compound 1A. All data obtained with both analyzers provide a very good fit with theoretical isotopic patterns. Due to high mass accuracy of QqTOF analyzer, we evaluated all isotopic masses and obtained mass errors (mass accuracies) for all isotopic peaks (m/z_{exp}) by the comparison with theoretical calculated exact masses (m/z_{theor}].

$$mass\ error = mass\ accuracy = 10^6 * \frac{m/z_{\exp} - m/z_{theor}}{m/z_{theor}}$$

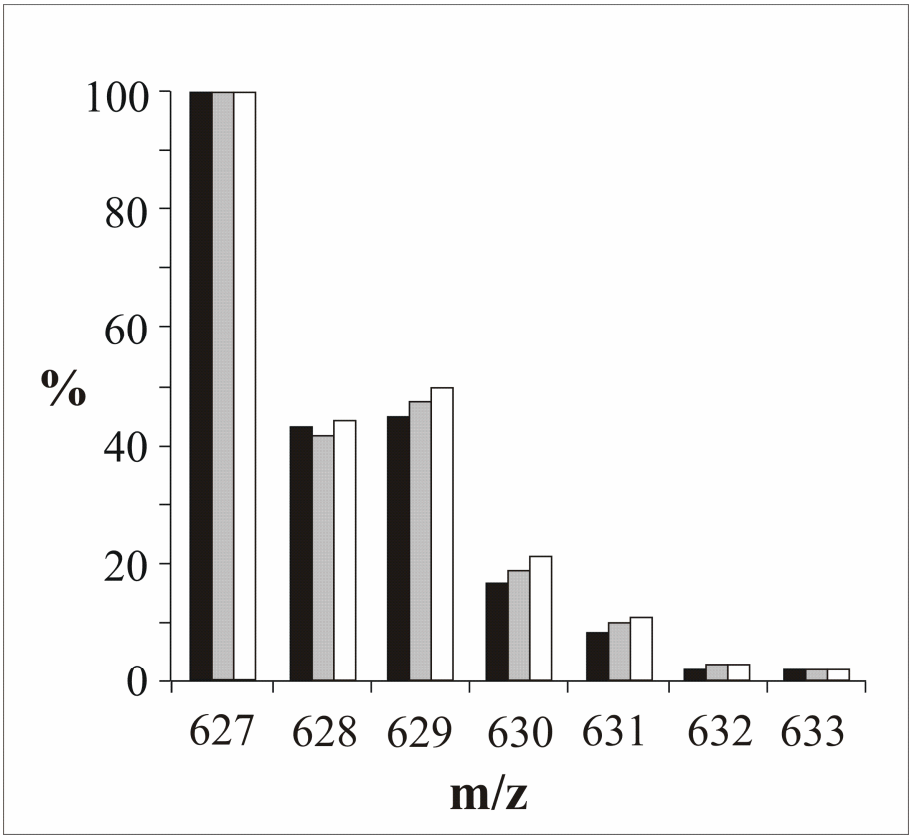

Figure 4.4.4 Comparison of experimental (ion trap - black bars, QqTOF - gray bars) and theoretical (white bars) isotopic abundances for protonated molecule of compound **1A**.

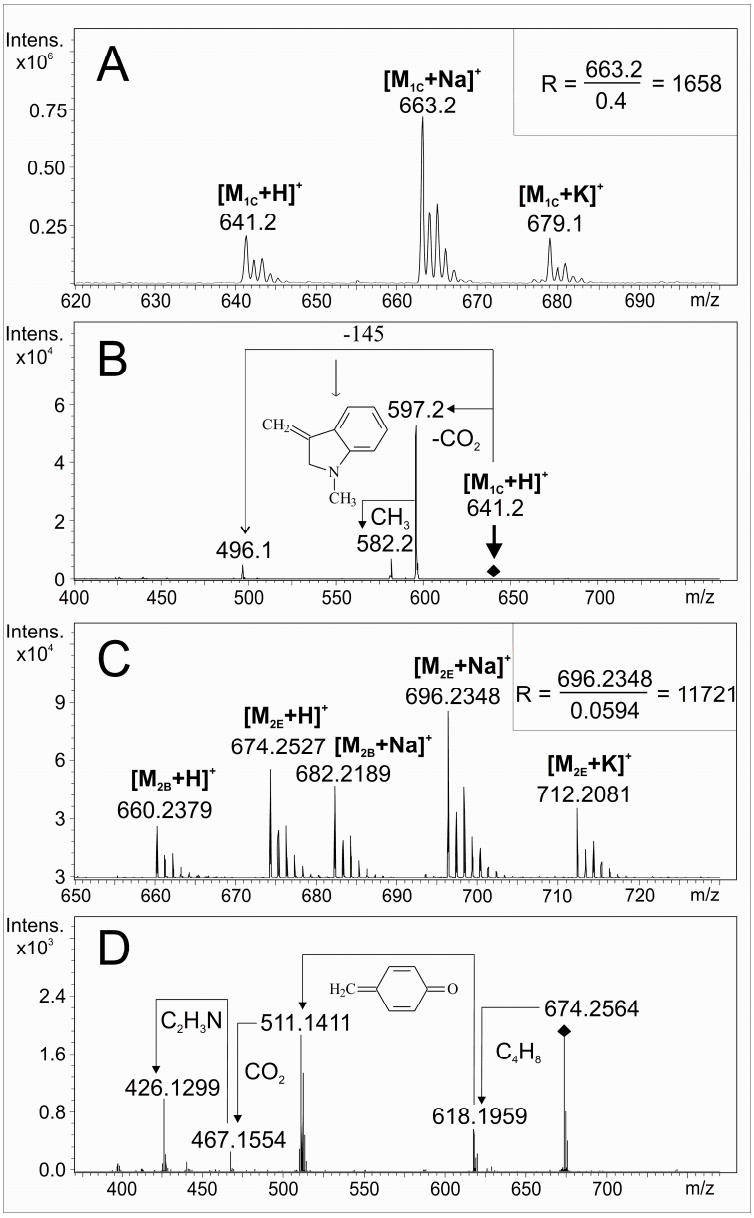

Figure 4.4.5 A/ Zoom of ion trap full scan positive-ion ESI mass spectra for methylation product **1C** with the calculated resolution, B/ Tandem mass spectrum of protonated molecule of **1C** (collision energy 0.8 V; isolation width Δ*m/z* 6)**,** C/ Zoom of QqTOF full scan positive-ion ESI mass spectra for methylation product **2E** with the calculated resolution, D/ Tandem mass spectrum of protonated molecules of **2E** (collision energy 25 eV/z; isolation width Δ*m/z* 6).

Further, absolute and relative mean mass errors are calculated which is the intensity (I_i) weighted mean absolute or relative deviation (err_i) between measured masses and theoretical masses of all peaks (n is the number of isotopes).

$$absolute\ mean\ mass\ error = \frac{|err_1| * I_1 + |err_2| * I_2 + \cdots + |err_n| * I_n}{\sum_{i=1}^{n} I_i}$$

It is worthy to point out the difference between the relative and absolute mean mass accuracies. The relative mean mass accuracy is calculated as the mean of mass accuracies of all isotopes including plus/minus sign, while the absolute mean mass accuracy is the mean of absolute values of mass accuracies. Let suppose a simple example of isotopic distribution containing only two ions with mass accuracies +3 ppm and -3 ppm, then the relative mean mass accuracy is 0 ppm, while the absolute mean mass accuracy is 3 ppm. Each parameter has different information content, the relative value should have very low values on condition that the mass calibration is precise, without a systematic error and real mass errors have random distribution. On the other hand, the absolute mean mass accuracy is the average difference between theoretical and experimental *m/z* values not regarding the sign, therefore much lower convergence to zero is expected. In general, worse accuracies may be expected for low abundant isotopic peaks which is treated by considering the relative abundances in the calculation algorithm. Both mean values can be strongly affected by the overlap with interfering ions, as discussed later on the example of $[M+Na]^+$ of **2E**.

A sigma value is used for individual ions as the combined value of the standard deviation of relative abundances for all peaks in the isotopic cluster from theoretical values [37]. The correct determination of the elemental composition of individual ions is even more reliable, when all isotopes considering their relative abundances are taken into account comparing to the established approach using only the most abundant isotopic ion. Typically, the sigma values lower than 0.05 predict the possibility of correct hit, mostly experimental sigma values are bellow 0.02 for the right elemental composition. On the other hand, values higher than 0.10 are considered as a strong indication that the suggested elemental composition is not correct or the interference is present. In our case, the worst mean mass accuracy of sodium molecular adduct with theoretical monoisotopic mass *m/z* 696.2343 for compound 2E is caused by the interference of the isotopic peak M^{+2} with monoisotopic mass *m/z* 698.1926 corresponding to the potassium molecular adduct of compound 2B. The resolution deducted from the spectrum (Fig. 4.4.5) is equal to 11721 which is deficient to resolve these two ions and hence only an envelope formed by the superposition of particular isotopes shifting the correct mass is observed. However, the mass accuracy of the first and second isotopes for $[M_{2E}+Na]^+$ is bellow 1 ppm (0.7 and 0.3 ppm), because the isotopic distribution is affected by superposition of $[M_{2B}+K]^+$ starting from the third isotope (*m/z* 698.2320).

The presence or absence of a protective group on the aromatic nitrogen (for tryptophan) or oxygen (for tyrosine) is easily recognized based on the determination of the molecular weights. Furthermore, the presence of protective group is confirmed by typical neutral losses associated with this group (Δ*m/z* 56 for butene or Δ*m/z* 100 for Boc protective group) observed in tandem mass spectra of $[M+H]^+$ (Fig. 4.4.6). The abundant ion at *m/z* 498 formed by the loss of stable conjugated system Δ*m/z* 129 is indication of tryptophan complex or Δ*m/z* 106 of tyrosine complex (see Fig. 4.4.6 for structures of neutral losses in agreement with [19]). This ion is also the base peak in MS/MS spectra of non-protected complexes and its structure is basically similar to the protonated molecule of glycine complex which was confirmed by the measurement of tandem mass spectra of glycine complex. The facile elimination of tryptophan (Fig. 4.4.6 **A**, **B**) and tyrosine (Fig. 4.4.6 **C**, **D**) side chains is similar as reported recently for ternary Cu(II) complexes [20, 21, 24]. Tandem mass spectra on both analyzers show identical

ions only differing in their relative abundances. The measurement of multistage mass spectra on the ion trap analyzer provides more structural information for studying the fragmentation paths (Fig. 4.4.7a-c), as illustrated on the fragmentation scheme of ion at *m/z* 498 suggested on the basis of detailed interpretation of MS^n spectra (Fig. 4.4.8). All suggested fragmentation paths are confirmed by the measurement of individual MS^n spectra step by step. All observed ions are singly charged, some of them are radical ions, as indicated in this figure.

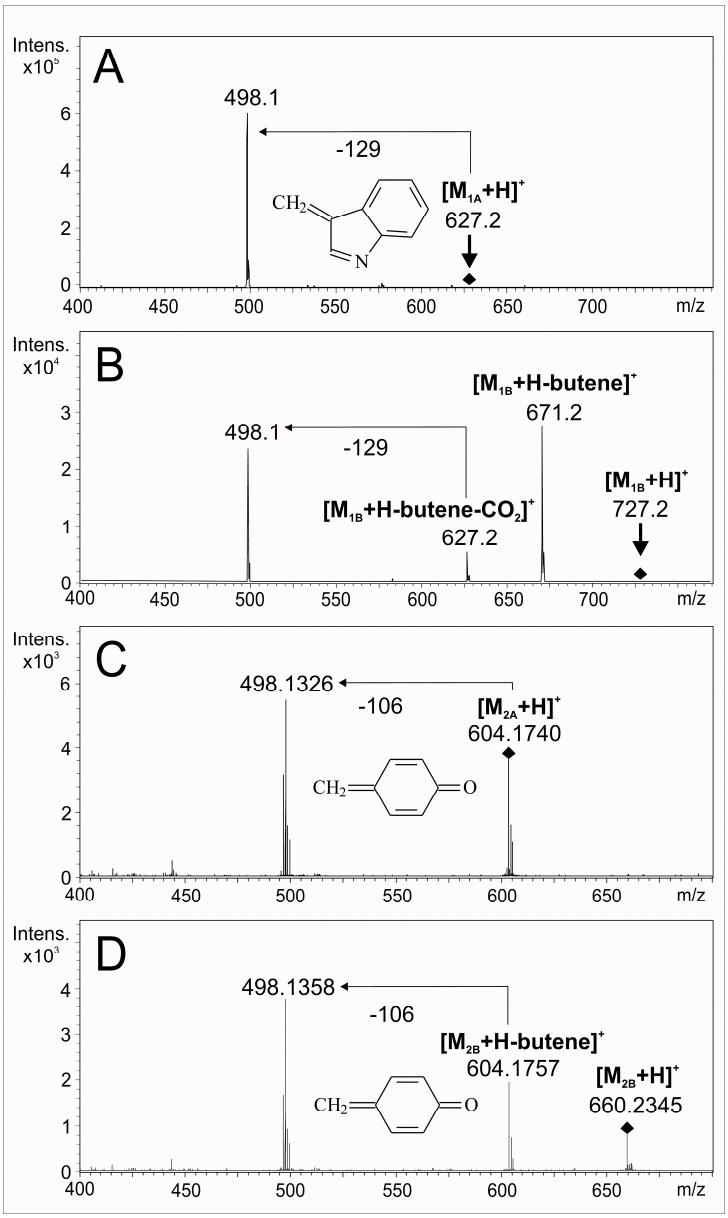

Figure 4.4.6 Tandem mass spectra of protonated molecules: A/ ion trap spectrum of compound **1A** (collision energy 0.8 V; isolation width Δ*m/z* 6), B/ ion trap spectrum of compound **1B** (collision energy 0.9 V; isolation width Δ*m/z* 6), C/ QqTOF spectrum of compound **2A**

(collision energy 25 eV/z; isolation width Δ*m/z* 6), D/ QqTOF spectrum of compound **2B** (collision energy 30 eV/z; isolation width Δ*m/z* 6).

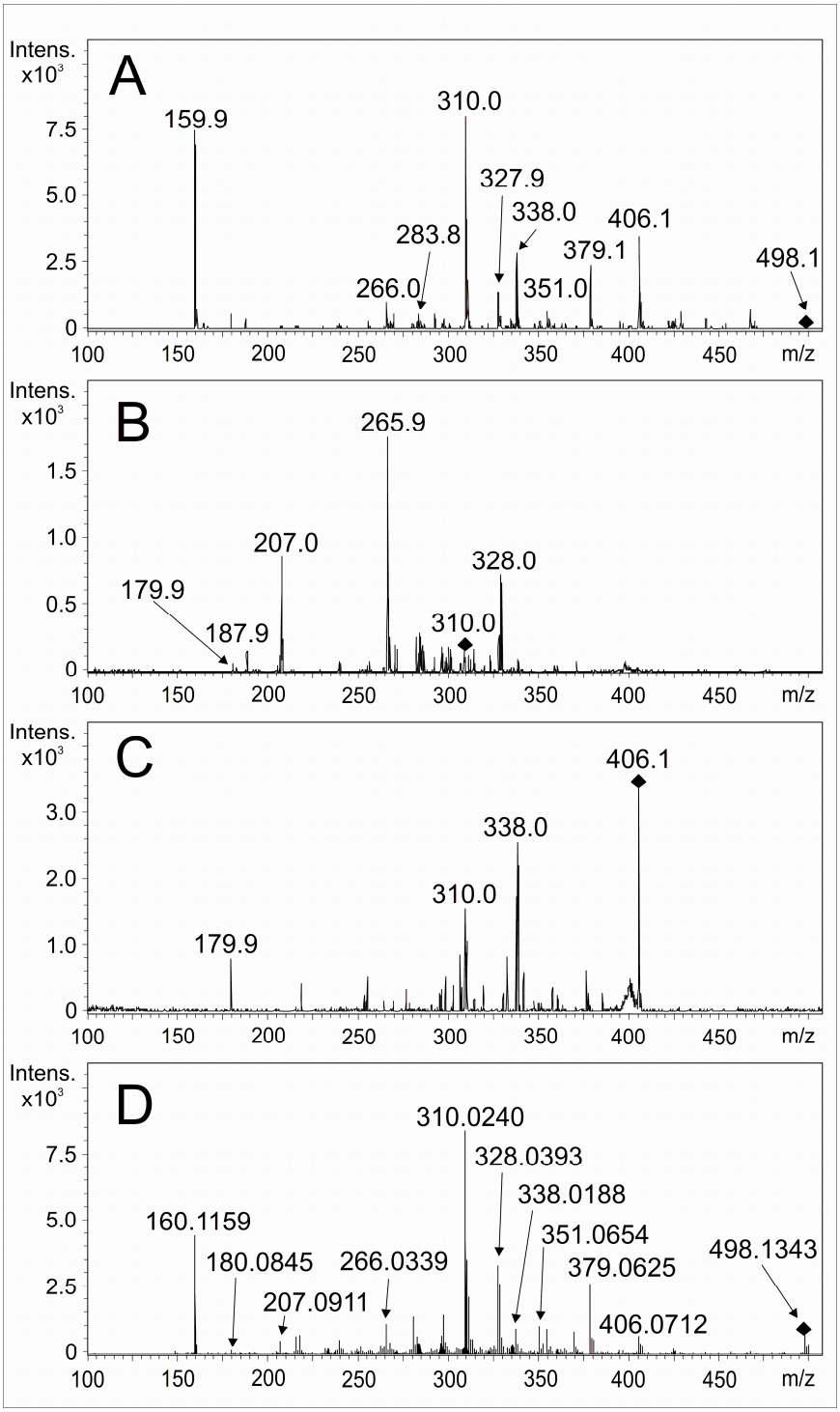

Figure 4.4.7 Tandem mass spectra of compound **1A**: A/ ion trap MS^3 spectrum of fragmentation path m/z 627 – 498 (collision energy 0.8 V; isolation width Δm/z 6), B/ ion trap

MS^4 spectrum of fragmentation path m/z 627 – 498 – 310 (collision energy 0.8 V; isolation width Δm/z 6), C/ ion trap MS^4 spectrum of fragmentation path m/z 627 – 498 – 406 (collision energy 0.8 V; isolation width Δm/z 6), D/ QqTOF in-source collision induced dissociation followed by MS^2 spectrum of m/z 498 (collision energy 30 eV/z; isolation width Δm/z 6). Suggested structures of observed ions are shown in the fragmentation scheme in Fig. 8.

The QqTOF analyzer enables mass spectra measurements only up to MS^2. The formation of fragment ions in MS/MS spectra depends on the collision induced dissociation (CID) which may be also performed in the source without the isolation step (in-source CID). When the in-source CID energy value is increased from 0 eV/z to 150 eV/z, then the peaks corresponding to $[M+H]^+$/$[M-H]^-$ ions have reduced relative abundances at cost of increased relative abundances of product ions (e.g. *m/z* 498). Subsequently, MS/MS spectrum of *m/z* 498 can be recorded. The overall appearance of this spectrum is very close to the ion trap MS^3 spectrum (Fig. 4.4.7d) but providing high mass accuracy applicable for the elemental composition determination.
Further, the methylation of protected complexes has been performed. Fig. 4.4.2 shows three possible products which may be formed by the methylation. The structures **1E** and **2E** correspond to the situation when the protective group is still present on the heteroatoms and the methylation is successfully carried out on desired α-methyl carbon of amino acids. However, during harsh conditions of methylation procedure, the complex may be deprotected and the methyl group can attack the heterocyclic nitrogen or oxygen (structures **1C** and **2C**). The last hypothetical possibility is that the complex is deprotected but the methylation is still successful (structures **1D** and **2D**). Mass spectrometric results make possible to exactly describe the reaction course of methylation which is reported for the first time. It is evident from ions observed in the full scan positive-ion mass spectrum of methylated tryptophan complex (Fig. 4.4.5a) that the complex is deprotected. Two structural possibilities with different methyl location still remain. Due to the same molecular weights, it is impossible to reveal the correct one based on the molecular weights only. It is necessary to search for the diagnostic product ions in MS/MS to distinguish between two possibilities. The MS/MS spectrum of protonated molecule at *m/z* 641 is shown in Fig. 4.4.5b. In case of methyl group bonded to the desired α-carbon of amino acid, the side-chain of complex is identical as for compound **1A**. The supposed neutral loss of this complex would be probably formed also by the loss of very stable conjugated system corresponding to Δ*m/z* 129. However, the different neutral losses (CO_2 and Δ*m/z* 145) are observed in the spectra, which is explained by the fact that the formation of stable conjugated system is affected by the presence of methyl group on the nitrogen, and then the neutral loss of carbon dioxide is preferred. Second, the loss of Δ*m/z* 145 is explained by the loss of side chain of **1C** (Fig. 4.4.2). Consequently, it can be concluded that the methylation has occurred at the nitrogen atom. Under harsh reaction conditions of methylation, the compounds are deprotected and the methylation leads to pure *N*-methylated products without any traces of *C*-methylation.
In case of the complex derived from *O*-methylated tyrosine, the protective group is stable enough and ions corresponding to *C*-methylated product are accompanied by ions of protected tyrosine complex without methylation (i.e. starting compound) in the full scan positive-ion spectra (Fig. 4.4.5c). The elemental composition is confirmed by QqTOF data. MS/MS spectrum of $[M_{2E}+H]^+$ ion provides information about successful methylation (Fig. 4.4.5d). The neutral loss associated with the presence of methyl group on the heteroatom (oxygen) is

not observed. First, the neutral loss of protective *tert*-butyl group is found. However, methyl presence on the desired α-methyl carbon of amino acid leads to the formation of radical ion at *m/z* 511 by the loss of Δ*m/z* 107 in comparison to non-methylated tyrosine complex with Δ*m/z* 106. The losses of carbon dioxide and C_2H_3N are also recognized in the spectrum probably due to the presence of methyl group. Based on above discussed interpretation, the success of α-methylation is confirmed (Fig. 4.4.2 - structure 2E).

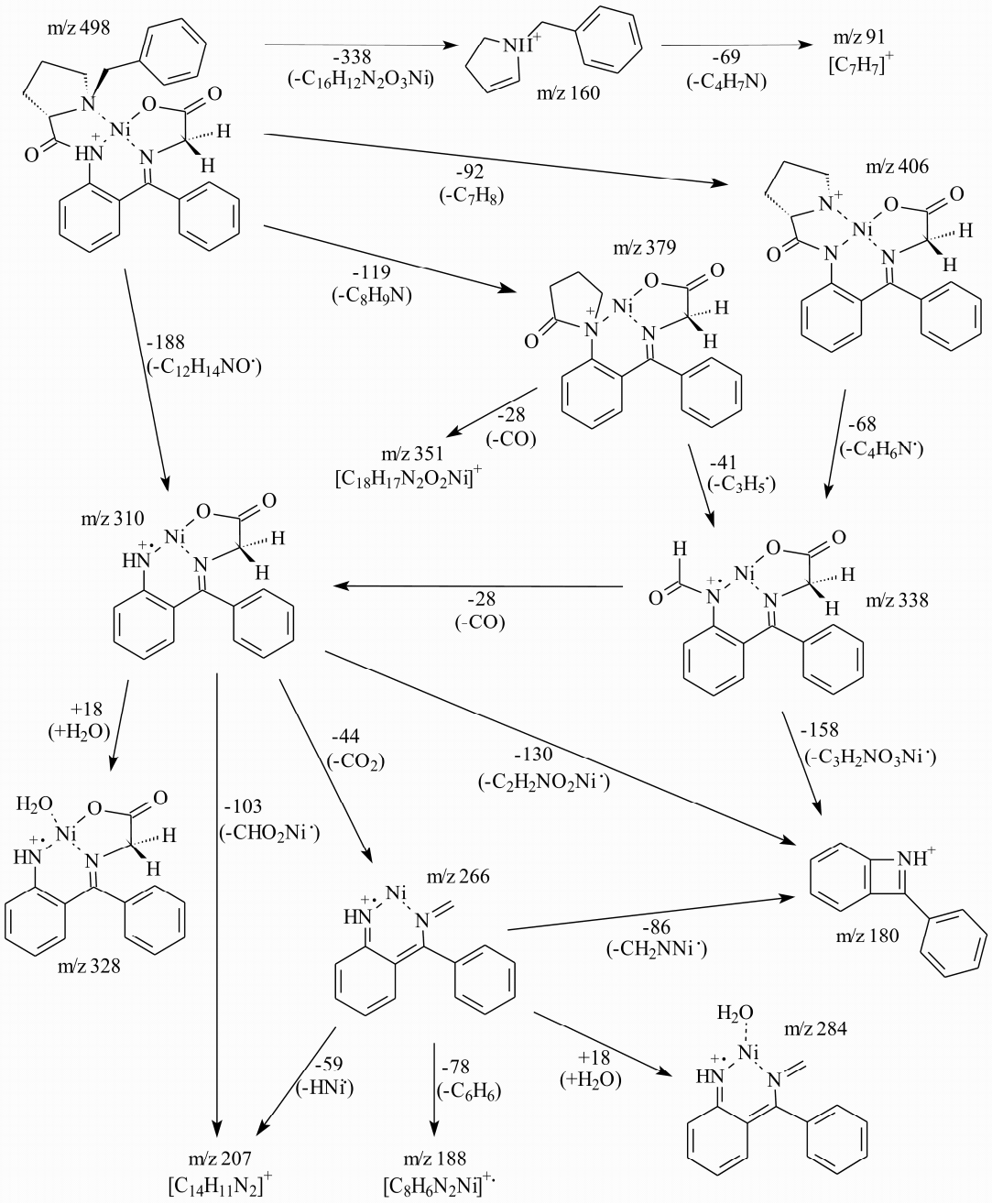

Figure 4.4.8 Suggested fragmentation pattern of $[M+H]^+$ ion at *m/z* 498 based on ion trap ESI-MS^n analysis and QqTOF verification of accurate masses for compound **1A**.

The elemental composition of all ions and all neutral losses shown in Fig. 4.4.8 were clearly confirmed by high mass accuracy measurements to avoid any speculation in cases of more potential interpretations, *e.g.* neutral losses of CO vs. CH_2CH_2. To confirm the proposed fragmentation scheme, several independent experiments were performed: a/ measurements in perdeuterated solvent (i.e. CD_3OD) to obtain $[M+D]^+$ because of better localization of protonation site in subsequent MS^n experiments, b/ MS^n of $[M+Na]^+$ ion, c/ MS^n of three isotopically labeled standards in the following positions ^{15}N3, ^{13}C19 and ^{13}C20 for the confirmation of suggested fragmentation scheme. The localization of the most probable protonation site is based on the comparison of MS^n of $[M+D]^+$ with non-labeled compound. The mass shift +1 related to one deuterium is observed for following ions and their products: *m/z* 406, 379, 338, 328, 310 and 266. On the other hand, no change is observed for *m/z* 160 and 91. Considering that the protonation should be placed on the most basic center in the molecule, two reasonable possibilities still remain, nitrogen atoms N2 and N3 (see numbering in Fig. 4.4.1). The distinguishing between these possibilities can be done with the help of the product ion *m/z* 180 containing only N2 and is clearly shifted to *m/z* 181 which suggests that the most probable protonation site is at N2, as indicated in Fig. 4.4.8. The question whether the ion m/z 180 really contains N2 but not N3 is answered by the measurement of ^{15}N3 labeled standard, where the loss of labeled ^{15}N3 is observed in the fragmentation step from *m/z* 267 to *m/z* 180. The experiment with MS^n of $[M+Na]^+$ ion provided comparable results as for $[M+D]^+$, i.e. no shift for *m/z* 160 and 91 and the mass shift of 22 *m/z* units for ions m/z 406, 310, 338, 266 and 207. Some less abundant ions (*m/z* 379, 328, 284 and 180) were not detected in this experiment with $[M+Na]^+$ because of sensitivity limitation with the sodium adduct. It seems probable that the sodium adduct formation also takes place at N2, but there is no experimental proof to reject the second alternative of N3 because of the lack of sensitivity.

MS^n experiments with three labeled standards at positions ^{15}N3, ^{13}C19 and ^{13}C20 confirmed that all ions proposed in Fig. 4.4.8 are in agreement with these spectra. Nitrogen ^{15}N3 is present in ions at *m/z* 406, 338, 328, 310, 284, 266, 207, and absent in ions *m/z* 180, 160 and 91. Carbon ^{13}C19 is observed in ions at *m/z* 406, 338, 328, 310, 284, 266, 207, and absent in m/z 180, 160 and 91. Carbon ^{13}C20 is detected only in the following ions: m/z 406, 338, 328 and 310. The important information is that ^{13}C20 is retained in the structure during the loss of CO from m/z 338 to m/z 310, but it is lost in the fragmentation step from m/z 310 to m/z 266 corresponding to the neutral loss of CO_2 in agreement with Fig. 4.4.8.

The typical feature of ESI mass spectra of Cu(II) complexes with amino acids [25-27] and small peptides [28, 29] is the formation of radical ions which may be then used for the generation of radical ion of amino acid itself for further gas-phase studies [19-24]. The behavior is less pronounced in case of Ni(II), which may be explained by the fact that copper has two common oxidation states Cu(II)/Cu(I) and hence it exhibits redox properties unlike Ni(II) with only one common oxidation state Ni(II). The radical ions in the spectra of Ni(II) are apparent only in MS^n spectra but not for ions in the molecular region. In some cases, the even electron ion is accompanied by a radical ion with lower relative intensity, for example the base peak *m/z* 498 in Figs. 4.4.6**C** and 4.4.6**D** is accompanied by the radical at *m/z* 497 with relative intensities 57% and 44%, respectively. The only logical explanation of the formation of *m/z* 497 is the radical loss of tyrosine side chain from $[M_{2A}+H]^+$ in Fig. 4.4.6C and from $[M_{2B}+H\text{-butene}]^+$ in Fig. 4.4.6D. The interesting difference is between ion trap (Figs. 4.4.6A, B) and QqTOF (Figs. 4.4.6C, D) MS/MS spectra, because the radical ion m/z is completely missing in

the ion trap spectra, while it has notable abundances in QqTOF spectra, which may be probably caused by longer reaction time in the trap (milliseconds) in comparison to QqTOF (microseconds).
The addition of small neutral oxygen containing species to the fragment ion in the trap after the loss the substituent bonded to the central metal atom is already known from the previous study of other organometallic complexes, where the addition of O_2 complemented two lost substituents on the central Co(III) atom [38]. In our case, the radical ion m/z 310 formed by the loss of the side radical chain on the central Ni(II) atom is replaced by the addition of H_2O during the isolation of this ion in the trap. The same example is the path from *m/z* 266 to *m/z* 284.

Conclusions

The complementary information from tandem mass spectra measured by two analyzer types, ion trap and QqTOF, is used for the structural characterization of Ni (II) complexes with Schiff bases of amino acids. The advantage of high-resolution QqTOF analyzer is the determination of accurate *m/z* values with mass accuracies better than 3 ppm even with the external calibration which is sufficient for the unambiguous determination of elemental composition and also for the true isotopic pattern recognition. Our approach implements the use of mass accuracies and relative abundances of all isotopes in the isotopic clusters containing a metal element. This combined information about all isotopes (*i.e.* relative and absolute mean mass accuracies) gives more reliable data in comparison to the conventional approach based on the most abundant isotopic peak only. Other supplementary information is the comparison of theoretical and experimental isotopic patterns for all proposed elemental combinations expressed as the sigma value. The ion trap analyzer is useful for the verification of the presence of polyisotopic elements and mainly for multistage tandem mass spectra measurements important for understanding the whole fragmentation patterns. The presented comprehensive approach is worthy especially in the structural analysis of molecules containing complex polyisotopic elements (e.g. metals), but in principle it is applicable for any organic, bioorganic and organometallic species.

Acknowledgements

This work was supported by the projects MSM0021627502 sponsored by the Ministry of Education, Youth and Sports of the Czech Republic and 203/08/1536 sponsored by the Grant Agency of the Czech Republic is acknowledged. M.N. acknowledges the support of the project VZ0021627501 sponsored by the Ministry of Education, Youth and Sports of the Czech Republic.

References

1. Belokon YN. Chiral complexes of Ni(II), Cu(II) and Cu(I) as reagents, catalysts and receptors for asymmetric-synthesis and chiral recognition of amino acids. Pure Appl. Chem. 1992; 64: 1917.
2. Debache A, Collet S, Bauchat P, Danion D, Euzenat L, Hercouet A, Carboni B. Belokon's Ni(II) complex as a chiral masked glycine for the diastereoselective synthesis of 2-substituted 1-aminocyclopropane carboxylic acids. Tetrahedron: Asymmetry 2001; 12: 761.
3. Soloshonok VA, Cai C, Yamada T, Ueki H, Ohfune Y, Hruby VJ. Michael addition reactions between chiral equivalents of a nucleophilic glycine and (S)- or (R)-3-[(E)-Enoyl]-4-

phenyl-1,3-oxazolidin-2-ones as a general method for efficient preparation of beta-substituted pyroglutamic acids. Case of topographically controlled stereoselectivity. J. Am. Chem. Soc. 2005; 127: 15296.
4. Vadon-Legoff S, Dijols S, Mansky D, Boucher JL. Improved and high yield synthesis of the potent arginase inhibitor: 2(S)-amino-6-boronohexanoic acid. Org. Process Res. & Develop. 2005; 9: 677.
5. Saghiyan AS, Geolchanyan AV. Asymmetric synthesis of all possible stereomers of 4-aminoglutamic acid via Michael condensation of chiral Ni(II) complexes of glycine and dehydroalanine. Synth. Commun. 2006; 36: 3667.
6. Saghiyan AS, Dadayan SA, Petrosyan SG, Manasyan LL, Geolchanyan AV, Djamgaryan SM, Andreasyan SA, Maleev VI, Khrustalev VN. New chiral Ni-II complexes of Schiff's bases of glycine and alanine for efficient asymmetric synthesis of α-amino acids. Tetrahedron: Asymmetry 2006; 17: 455.
7. Soloshonok VA, Ueki H. Design, synthesis, and characterization of binuclear Ni(II) complexes with inherent helical chirality. J. Am. Chem. Soc. 2007; 129: 2426.
8. Belokon YN, Bakhmutov VI, Chernoglazova NI, Kochetkov KA, Vitt SV, Garbalinskaya NS, Belikov VM. General method for the asymmetric synthesis of α-amino acids via alkylation of the chiral nickel(II) Schiff base complexes of glycine and alanine. J. Chem. Soc, Perkin Trans. 1 1988; 2: 305.
9. Gu XY, Ndungu JA, Qiu W, Ying J, Carducci MD, Wooden H, Hruby VJ. Large scale enantiomeric synthesis, purification, and characterization of ω-unsaturated amino acids via a Gly-Ni(II)-BPB-complex. Tetrahedron 2004; 60: 8233.
10. Antoni G, Kihlberg T, Långström B. Aspects on the Synthesis of ^{11}C-Labelled Compounds (in Handbook of Radiopharmaceuticals, Welch M.J., Redvanly C.S., Wiley, Chichester, 2003), pp. 141-194.
11. Popkov A, Nádvorník M, Kružberská P, Lyčka A, Lehel S, Gillings NM. Towards stereoselective radiosynthesis of α-[^{11}C]methylsubstituted aromatic α-amino acids - a challenge of creation of quaternary asymmetric centre in a very short time. J. Labelled Compd. Radiopharm. 2007, 50: 374.
12. Nádvorník M, Popkov A. Improved synthesis of the Ni(II) complex of the Schiff base of (*S*)-2-[*N*-(*N*'-benzylprolyl)amino]benzophenone and glycine. Green Chemistry 2002, 4: 71.
13. Popkov A, Gee A, Nádvorník M, Lyčka A. Chiral nucleophilic glycine and alanine synthons: nickel(II) complexes of Schiff bases of (S)-N-(2,4,6-trimethylbenzyl)proline (2-benzoylphenyl)amide and glycine or alanine. Transition Met. Chem., 2002; 27: 884.
14. Popkov A, Langer V, Manorik PA, Weidlich T. Long-range spin-spin interactions in the C-13-NMRspectra of the nickel(II) complex of the Schiff base of (S)-N-benzylproline (2-benzoylphenyl)amide and glycine. Quantum-chemical calculations and possible donation of electron density from the π-system of the benzyl group to nickel. Transition Met. Chem. 2003; 28: 475.
15. Langer V, Popkov A, Nádvorník M, Lyčka A. Two new Ni(II) Schiff base complexes: X-ray absolute structure determination, synthesis of a ^{15}N-labelled complex and full assignment of its ^{1}H NMR and ^{13}C NMR spectra. Polyhedron. 2007, 26: 911.
16. Vaisar T, Gatlin CL, Rao RD, Seymour JL, Tureček F. Sequence information, distinction and quantitation of C-terminal leucine and isoleucine in ternary complexes of tripeptides with Cu(II) and 2,2-' bipyridine. J. Mass Spectrom. 2001; 36: 306-316.

17. Lagarrigue M, Bossee A, Afonso C, Fournier F, Bellier B, Tabet JC. Diastereomeric differentiation of peptides with CuII and FeII complexation in an ion trap mass spectrometer. J. Mass Spectrom. 2006; 41: 1073-1085.
18. Zhang DX, Tao WA, Cooks RG. Chiral resolution of D- and L-amino acids by tandem mass spectrometry of Ni(II)-bound trimeric complexes. Int. J. Mass Spectrom. 2001; 204: 159-169.
19. Bagheri-Majdi E, Ke YY, Orlova G, Chu IK, Hopkinson AC, Siu KWM. Copper-mediated peptide radical ions in the gas phase. J. Phys. Chem. B 2004; 108: 11170.
20. Chu IK, Rodriquez CF, Lau TC, Hopkinson AC, Siu KWM. Molecular radical cations of oligopeptides. J. Phys. Chem. B 2000; 104: 3393.
21. Barlow CK, Moran D, Radom L, McFadyen WD, O'Hair RAJ. Metal-mediated formation of gas-phase amino acid radical cations. J. Phys. Chem. A 2006; 110: 8304.
22. Wee S, O'Hair RAJ, McFadyen WD. Side-chain radical losses from radical cations allows distinction of leucine and isoleucine residues in the isomeric peptides Gly-XXX-Arg. Rapid. Commun. Mass Spectrom. 2002; 16: 884.
23. Lam CNW, Ruan EDL, Ma CY, Chu IK. Non-zwitterionic structures of aliphatic-only peptides mediated the formation and dissociation of gas phase radical cations. J. Mass Spectrom. 2006; 41: 931.
24. Barlow CK, Wee S, McFadyen WD, O'Hair RAJ. Designing copper(II) ternary complexes to generate radical cations of peptides in the gas phase: Role of the auxiliary ligand. Dalton Trans.2004; 20: 3199.
25. Gatlin CL, Tureček F, Vaisar T. Copper(II) amino-acid complexes in the gas-phase. J. Am. Chem. Soc. 1995; 117: 3637.
26. Gatlin CL, Tureček F, Vaisar T. Gas-phase complexes of amino-acids with Cu(II) and diimine ligands. 1. aliphatic and aromatic-amino-acids. J. Mass Spectrom. 1995; 30: 1605.
27. Gatlin CL, Tureček F, Vaisar T. Gas-phase complexes of amino-acids with Cu(II) and diimine ligands. 2. amino-acids with o, n and s functional-groups in the side-chain. J. Mass Spectrom. 1995; 30: 1617.
28. Gatlin CL, Rao RD, Turecek F, Vaisar T. Carboxylate and amine terminus directed fragmentations in gaseous dipeptide complexes with copper(II) and diimine ligands formed by electrospray. Anal. Chem. 1996; 68: 263.
29. Vaisar T, Gatlin CL, Turecek F. Oxidation of peptide-copper complexes by alkali metal cations in the gas phase. J. Am. Chem. Soc. 1996; 118: 5314.
30. Vaisar T, Gatlin CL, Turecek F. Metal-ligand redox reactions in gas-phase quaternary peptide-metal complexes by electrospray ionization mass spectrometry. Int. J. Mass Spectrom. Ion Processes 1997; 162: 77.
31. Denekamp C. Rabkin E. Radical Induced Fragmentation of amino acids esters using triphenylcorrole (CuIII) complexes. J. Am. Soc. Mass Spectrom. 2007; 18: 791.
32. Řehulka P, Popkov A, Nádvornik M, Planeta J, Mazanec K, Chmelik J. Off-line combination of reversed-phase liquid chromatography and laser desorption/ionization time-of-flight mass spectrometry with seamless post-source decay fragment ion analysis for characterization of square-planar nickel(II) complexes. J. Mass Spectrom. 2006; 41: 448.
33. Kolářová L, Holčapek M, Jambor R, Dostál L, Nádvorník M, Růžička A. Structural analysis of 2,6-[bis(alkyloxy)methyl]phenyltin derivatives using electrospray ionization mass spectrometry. J. Mass Spectrom. 2004; 39: 621.

34. Holčapek M, Kolářová L, Růžička A, Jambor R, Jandera P. Structural analysis of ionic organotin(IV) compounds using electrospray tandem mass spectrometry. Anal. Chem. 2006; 78: 4210.
35. Jirásko R, Holčapek M, Kolářová L, Basu Baul TS. Electrospray ionization-multistage tandem mass spectrometry of complex multitin organometallic compounds. J. Mass Spectrom. 2007; 42: 918.
36. Wei J, Chen J, Miller JM. Electrospray ionization mass spectrometry of organogermanium compounds. Rapid. Commun. Mass Spectrom. 2001; 15: 169.
37. Ojanperä S, Pelander A, Pelzing M, Krebs I, Vuori E, Ojanperä I. Isotopic pattern and accurate mass determination in urine drug screening by liquid chromatography/time-of-flight mass spectrometry. Rapid. Commun. Mass Spectrom. 2006; 20: 1161.
38. Lemr K, Holčapek M, Jandera P. Oxygen Attachment to the Metal Complex Ions during their Collision Induced Dissociation in the Ion Trap. Rapid Commun. Mass Spectrom. 2000; 14: 1878.

Chapter 4.5

Towards Stereoselective Radiosynthesis of α-[^{11}C]Methylsubstituted Aromatic α-Amino Acids - a Challenge of Creation of Quaternary Asymmetric Centre in a Very Short Time

Alexander Popkov[1,5], Milan Nádvorník,[2] Pavla Kružberská,[3] Antonín Lyčka,[4] Szabolcs Lehel[5] and Nicholas Gillings[5]

[1] Faculty of Health and Social Studies, University of South Bohemia, Czech Republic, [2] Department of General and Inorganic Chemistry, University of Pardubice, Czech Republic, [3] Department of Analytical Biochemistry, Institute of Entomology, České Budejovice, Czech Republic, [4] Institute for Organic Syntheses, Rybitví, Czech Republic, [5] PET & Cyclotron Unit, Copenhagen University Hospital, Denmark

J. Label. Compd. Radiopharm. **2007**, *50*, 370

Summary

In positron emission tomography (PET) α-methyl amino acids have two potential applications:
1. as analogues of neutransmitter precursors for the study of neurodegenerative diseases,
2. as non-metabolised analogues of proteinogenic amino acids for the study of amino acid uptake into normal and cancer cells.
Clinical applications of such amino acids are strongly limited due to their poor availability.
We carried out [^{11}C]methylation of metallocomplex synthons derived from protected DOPA or tyrosine. For [^{11}C]methylation, sodium hydroxide (5 mg of fine dry powder) was sealed in a vial, which was flushed with dry nitrogen before addition of a solution of the complex (10 mg) and $^{11}CH_3I$ in 1,3-dimethylimidazolidin-2-one (300 µl). After 10 min at 25°C, a 9% radiochemical yield (decay corrected) of a mixture of the diastereomeric α-[^{11}C]methylDOPA complexes or a 7% radiochemical yield of a mixture of the diastereomeric α-[^{11}C]methyltyrosine complexes was achieved. Individual diastereomers were successfully separated by preparative HPLC, diluted with excess of water and extracted on C18 cartridges. Optimisation of the procedure including hydrolysis of the complexes (hydrolytic deprotection of enantiomerically pure amino acids) and subsequent purification of the enantiomers of α-[^{11}C]methylDOPA and α-[^{11}C]methyltyrosine is underway.

Keywords

asymmetric synthesis, α-methyl amino acids, carbon-11, [^{11}C]methylation, DOPA, tyrosine, nickel, complexes

Introduction

α-Amino acids bearing an α-methyl group are widely used for replacement of proteinogenic amino acids with their α-methylated analogues in peptides. Such modification of peptides introduces restriction to conformational freedom and increases stability of the peptides towards various enzymes. In positron emission tomography (PET) α-[^{11}C]methyl amino acids could play a dual role:

1. Precursors of neurotransmitters analogues for the study of neurodegenerative diseases.
2. Non-metabolised analogues of proteinogenic amino acids for the study of amino acids uptake into normal and cancer cells.[1]

Evaluation of the clinical usefulness of such amino acids is limited by the lack of reliable preparative approaches to these compounds. An industrial procedure was adopted for the synthesis of the only enantiomerically pure ^{11}C-labelled α-methyl amino acid, α-[^{11}C]methyltryptophan.[2] All attempts to prepare enantiomerically pure α-[^{11}C]methylated tyrosine failed.[3] The only published synthesis of ^{11}C-methyl labelled α-metyltyrosine utilised a very original combined chemical and enzymatic approach.[3a] The amino acid core was built by malonic ester chemistry; dimethyl 2-(4-methoxybenzyl)malonate was methylated with [^{11}C]methyliodide. Hydrolysis of the prochiral diester using pig liver esterase (EC 3.1.1.1) led to the enantiomerically enriched monoester. After transformation of the free carboxylic group into an amino group via isocyanate and deprotection, the labelled α-methyltyrosine was obtained in 62 % *e.e.* The decay-corrected radiochemical yield was 12-20% in a synthesis time of 45-50 min. However, low enantiomeric excess and long synthesis does not allow the use of this approach for rutine clinical production of the amino acid. Except for ^{11}C-labelled α-methyltryptophan and several ^{14}C-labelled α-methyl amino acids (α-methyltyrosine[4] and α-methylDOPA), no other enantiomerically pure radiolabelled α-methyl amino acid have been used for in vivo investigations in humans (α-[^{11}C]methyltryptophan) or laboratory animals.

Our efforts concentrated on adaptation of known metallocomplex amino acids synthons widely used for preparation of non-labelled α-methyl amino acids.[5] Ni(II) complexes of Schiff bases of (*S*)-*N*-benzylproline (2-benzoylphenyl)amide (BPB) and α-amino acids were developed as artificial analogues of pyridoxal 5'-phosphate (PLP)-dependent enzymes. BPB was designed as a re-usable enzyme-like chiral auxiliary. Their preparative applications for stoichiometric asymmetric synthesis of α-amino acids are being perfected by a number of groups worldwide.[6]

Results and Discussion

(^{13}C)Methylation of sterically hindered complexes derived from protected tyrosine and protected DOPA ((*S*,*S*)-TyrK, (*S*,*S*)-TyrK(OBu-t) and (*S*,*S*)-DOPAK, Scheme 4.5.1) by five-fold excess of $^{13}CH_3I$ was chosen as a model reaction. Alkylation in the aprotic solvent DMI run as expected for alkylation of sterically hindered tertiary carbon. Yields varied from experiment to experiment depending mostly on particle size and dryness of the KOH used.

For [^{11}C]methylation of (*S*,*S*)-DOPAK and (*S*,*S*)-TyrK(OBu-t), dry fine powdered KOH was sealed in a vial, the vial was flushed with dry argon followed by addition of a solution of the complex and $^{11}CH^3I$ in DMI (300 μl). After 10 min at 25°C, the 4% radiochemical yield of (*S*,*S*)-α-[^{11}C]methylDOPAK and 5% radiochemical yield of (*S*,*R*)-α-[^{11}C]methylDOPAK was achieved. Yield of diastereomers of α-[^{11}C]MeTyrK(OBu-*t*) was 7%. Low radiochemical yield was observed due to two reasons:

1. (*S*,*S*)-α-[^{11}C]MeDOPAK is a minor diastereomer. Sterically preferred *si*-attack leads to unwanted (*S*,*R*)-α-[^{11}C]MeDOPAK. This disadvantage might be overcome by application of the starting complex with opposite configuration of the asymmetric centres. Usage of the complexes derived from a new generation chiral auxiliaries[7] instead of BPB should further increase the yield of the desired diastereomer.

2. Slow alkylation of the sterically hindered α-carbon allows [^{11}C]methyl iodide to be mostly hydrolysed by KOH.

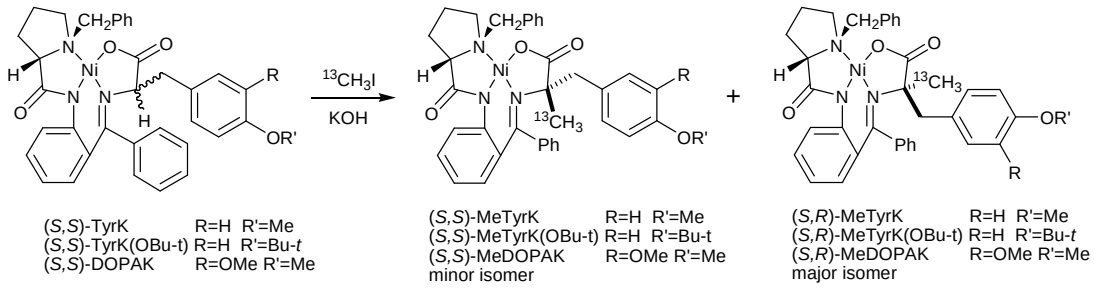

Scheme 4.5.1 (^{13}C)Methylation of the complexes

Chromatographic properties of (*S*,*S*)-α-MeTyrK and (*S*,*R*)-α-MeTyrK are very similar. Their separation on a 4 x 150 mm C18 column takes 50 min, too long a time for preparation of ^{11}C-labelled compounds. While useless for radiochemical syntheses, the complex was a convenient model for assignment of stereochemistry of the products of (^{13}C)methylation. Diastereomers of MeTyrK(OBu-*t*) or diastereomers of α-MeDOPAK are easily separable. The retention times of (*S*,*S*)-α-MeDOPAK and starting (*S*,*S*)-DOPAK are so close that the mixture of these compounds appears as a single peak on a chromatogram. This was elucidated by application of

the reconstructed ion current technique during HPLC-ESI-MS separation of a mixture of starting (*S*,*S*)-DOPAK and both (*S*,*R*)-α-(^{13}C)MeDOPAK and (*S*,*S*)-α-(^{13}C)MeDOPAK (Figure 4.5.2).

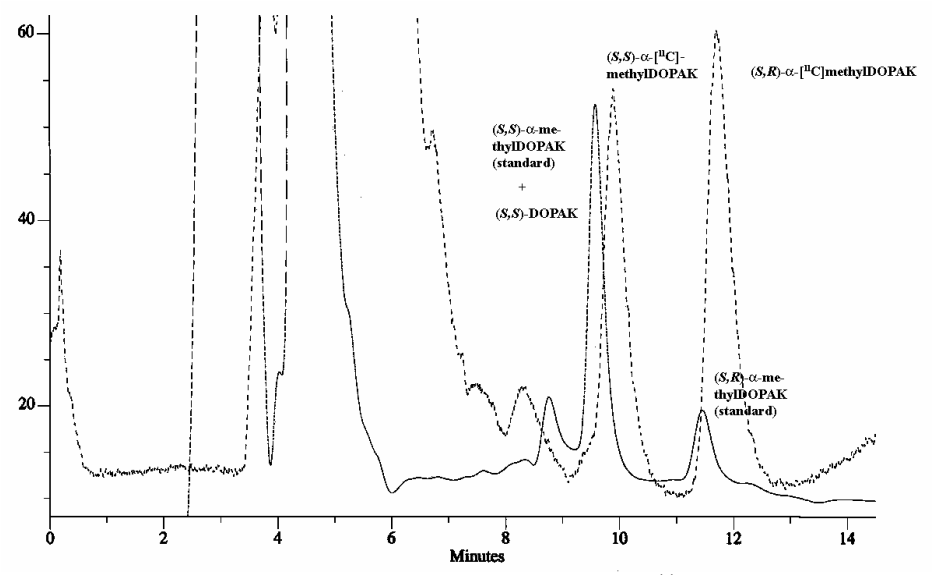

Figure 4.5.1 HPLC separation of diastereomers of α-[^{11}C]MeDOPAK (dotted line, detection by γ-detector); added standards – α-methylDOPAK diastereomers and (*S*,*S*)-DOPAK were detected by UV-detector (solid line)

Stereochemistry of the diastereomers of α-(^{13}C)MeTyrK was assigned by combined application of ^{13}C NMR and circular dichroism (CD) spectroscopy:
1. the reaction mixture after alkylation of (*S*,*S*)-TyrK with $^{13}CH_3I$ gave two predominant peaks in the ^{13}C NMR spectrum: minor at 29.3 ppm and major at 28.5 ppm. The diastereomeric excess was 7 %;
2. preparative TLC separation of the reaction mixture gave two fractions. In the ^{13}C NMR spectrum of the first fraction a single predominant peak at 29.3 ppm was recorded. The first fraction was associated with minor diastereomer. Similarly, in the ^{13}C NMR spectrum of the second fraction a single predominant peak at 28.5 ppm was recorded. The second fraction was associated with the major diastereomer;
3. circular dichroism spectra of starting (*S*,*S*)-TyrK and both fractions (diastereomers) of α-(^{13}C)MeTyrK were recorded. Cotton effects in the spectra of both (*S*,*S*)-TyrK and the first fraction (minor diastereomer) were similar in both areas (650-480 nm and 480-360 nm). Cotton effect in the spectrum of the second fraction (major diastereomer) in the range 480-360 nm had an opposite sign (Figure 3). Based on these CD data, the *SS* configuration was assigned to the first fraction (minor diastereomer) and the *SR* configuration was assigned to the second fraction (major diastereomer). This assignment is consistent with the proposed predominance of *si*-alkylation leading to (*S*,*R*)-α-(^{13}C)MeTyrK as the major product (Scheme 4.5.1).

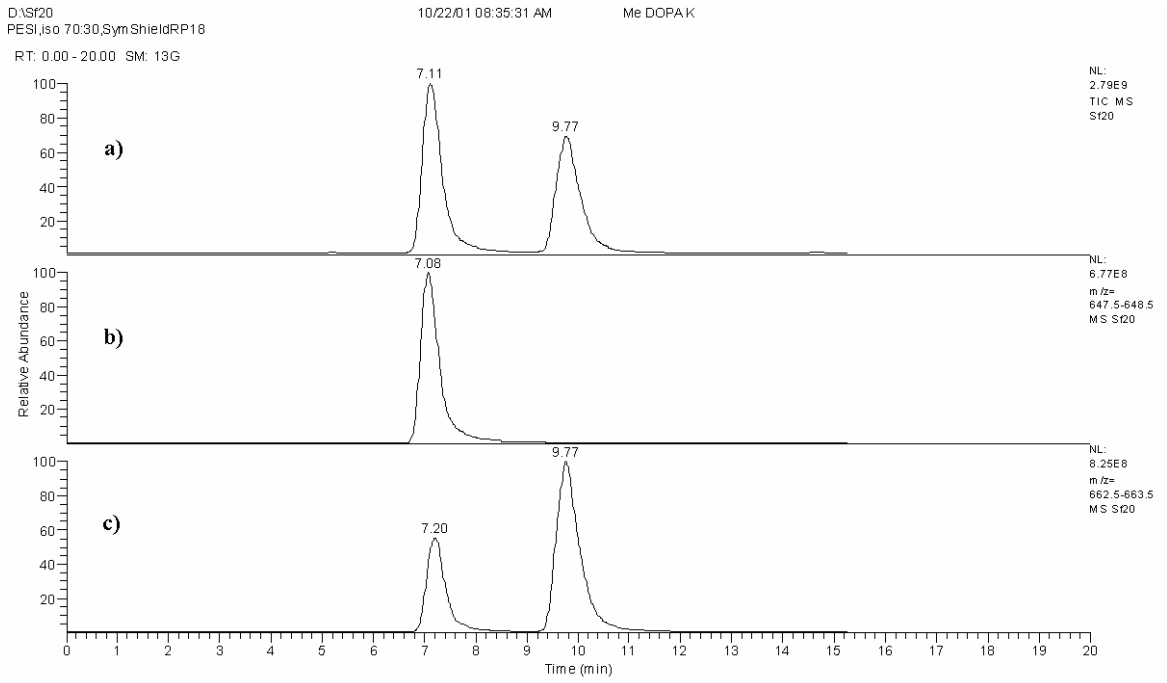

Figure 4.5.2 Reconstructed ion current (RIC) chromatogram during HPLC-ESI-MS separation of (*S*,*S*)-DOPAK ($[M]^+$=647) and both diastereomers of α-(^{13}C)MeDOPAK ($[M]^+$=663):
a) total ion current chromatogram (similar to HPLC analysis with UV-VIS detection);
b) RIC chromatogram (M=647.5-648.5). Retention time 7.08 min corresponds to (*S*,*S*)-DOPAK;
c) RIC chromatogram (M=662.5-663.5). Retention time 7.20 min corresponds to (*S*,*S*)-α-(^{13}C)MeDOPAK; retention time 9.77 min corresponds to (*S*,*R*)-α-(^{13}C)MeDOPAK.

The predominant signals in the ^{13}C NMR spectra of diastereomers of α-MeTyrK(OBu-*t*) and α-(^{13}C)MeDOPAK were assigned by analogy. In the case of α-MeDOPAK the major peak at 28.9 ppm was assigned to (*S*,*R*)-α-(^{13}C)MeDOPAK, the minor peak at 27.7 ppm was assigned to (*S*,*S*)-α-(^{13}C)MeDOPAK. The diastereomeric excess of the methylation reaction was 12 %. Higher diastereomeric excess is probably due to additional steric hindrance introduced by the second methoxy group in the amino acid part of the complex.
Individual diastereomers of α-[^{11}C]MeTyrK(OBu-*t*) and α-[^{11}C]MeDOPAK were successfully separated by preparative HPLC, diluted with excess of water and extracted on C18 cartridges. Optimisation of the procedure including hydrolysis of the complexes (hydrolytic deprotection of enantiomerically pure amino acids) and subsequent purification of the enantiomers of α-[^{11}C]methylDOPA and α-[^{11}C]methyltyrosine is underway.

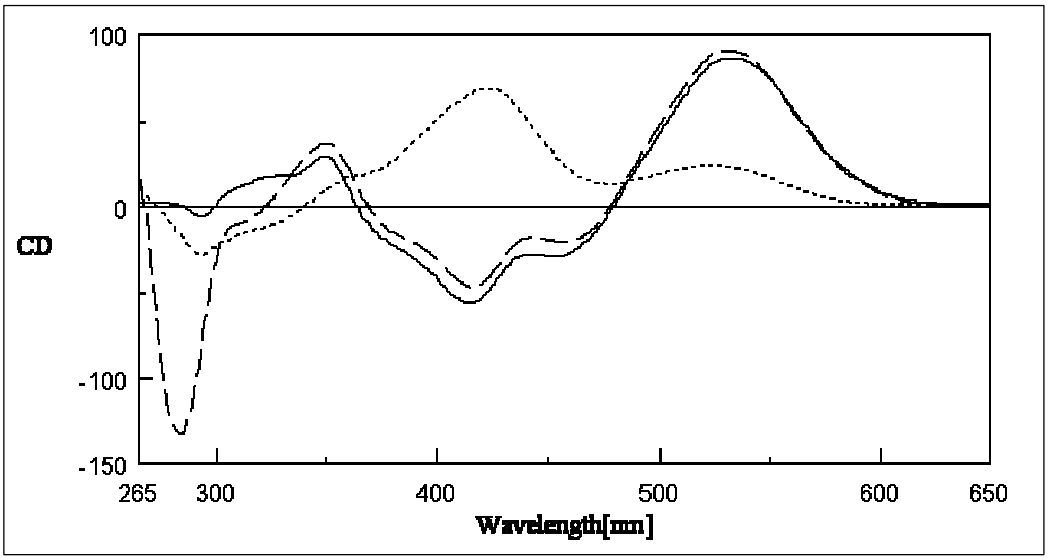

Figure 4.5.3 CD spectra of (*S*,*S*)-TyrK (——————), the first fraction, (*S*,*S*)-α-([13]C)MeTyrK (—— —— ——) and the second fraction (*S*,*R*)-α-([13]C)MeTyrK (• • • • • • •).

Conclusion

A synthetic procedure suitable for the routine preparation of (*S*)-α-[[11]C]methylDOPA and (*S*)-α-[[11]C]methyltyrosine was developed, final radiochemical synthetic steps are now being optimised.

Acknowledgements

Access to Jasco J-715 is acknowledged (grant MSM 6007665808).

References

1. Brogden RN, Heel RC, Speight TM, Avery GS, *Drugs*, 1981; **21**: 81.
2. (a) Crich D, Davies JW, *J. Chem. Soc., Chem. Commun*., 1989; 1418; (b) Bourne GT, Crich D, Davies JW, Horwell DC, *J. Chem. Soc., Perkin Trans.1*, 1991; 1693; (c) Plenevaux A, Lemaire C, Delfiore G, Comar D, *Appl. Radiat. Isot.* 1994; **45**: 651.
3. (a) Gee AD, Långström B, *J. Chem. Soc., Perkin Trans.* 1 1991; 215; (b) Rajagopal S, Venkatachalam TK, Conway T, Diksic M, *Appl. Radiat. Isot.* 1992; **43**: 979.
4. Cumming P, Venkatachalam TK, Rajagopal S, Diksic M, Gjedde A, *Synapse*, 1994; **17**: 125.
5. Belokon YN, Bakchmutov VI, Chernoglazova NI, Kochetkov KA, Vitt SV, Garbalinskaya NS, Belikov VM, *J. Chem. Soc., Perkin Trans.* 1 1988; 305 .
6. (a) Belokon YN, Bulychev AG, Vitt SV, Struchkov YT, Batsanov AS, Timofeeva TV, Tsyryapkin VA, Ryzhov MG, Lysova LA, Bakhmutov VI, Belikov VI, *J. Am. Chem. Soc.* 1985; **107**: 4252; (b) Belokon YN, *Pure Appl. Chem.* 1992; **64**: 1917; (c) Collet S, Bauchat P, Danion-Bougot R, Danion D, *Tetrahedron: Asymmetry* 1998; **9**: 2121; (d) Belokon YN, Tararov VI, Maleev VI, Saveleva TF, Ryzhov MG, *Tetrahedron: Asymmetry* 1998; **9**: 4249; (e) Qiu W, Soloshonok VA, Cai C, Tang X, Hruby VJ, *Tetrahedron* 2000; **56**: 2577; (f) Tang X., Soloshonok VA, Hruby VJ, *Tetrahedron: Asymmetry* 2000; **11**: 2917; (g) Cai

C, Soloshonok VA, Hruby VJ, *J. Org. Chem.* 2001; **66**: 1339; (h) Belokon YN, Kochetkov KA, Ikonnikov NS, Strelkova TV, Harutyunyan SR, Saghiyan AS, *Tetrahedron: Asymmetry* 2001; **12**: 481; (i) Debache A, Collet S, Bauchat P, Danion D, Euzenat L, Hercouet A, Carboni B, *Tetrahedron: Asymmetry* 2001; **12**: 761; (j) Popkov A, Císařová I, Sopková J, Jirman J, Lyčka A, Kochetkov KA, *Collect. Czech. Chem. Commun.* 2005; **70**: 1397.

7. (a) Popkov A, Gee A, Nádvorník M, Lyčka A, *Trans. Metal Chem*. 2002; **27**: 884; (b) Saghiyan AS, Hambardzumyan HH, Manasyan LL, Petrosyan AA, Maleev VI, Peregudov AS, *Synth. Commun.* 2005; **35**: 449.